Second and third order stresses,

TEM and SEM

(ESEM/EBSD measurements of surface microstrain fields)

Institute of Metallurgy and Materials Science, Polish Academy of Sciences, 25 Reymonta St., 30-059 Krakow, Poland.

Outline

1. Introduction
2. Orientation microscopy employed to local stress characterization
3. Surface strain characterization of alumina
4. Surface strain characterization of zirconia
5. Microstructure of polycrystalline zinc subjected to plastic deformation by complex loading.

Crystal Orientation Mapping

(Crystallographic orientation)

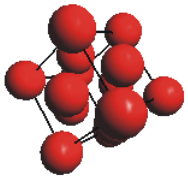

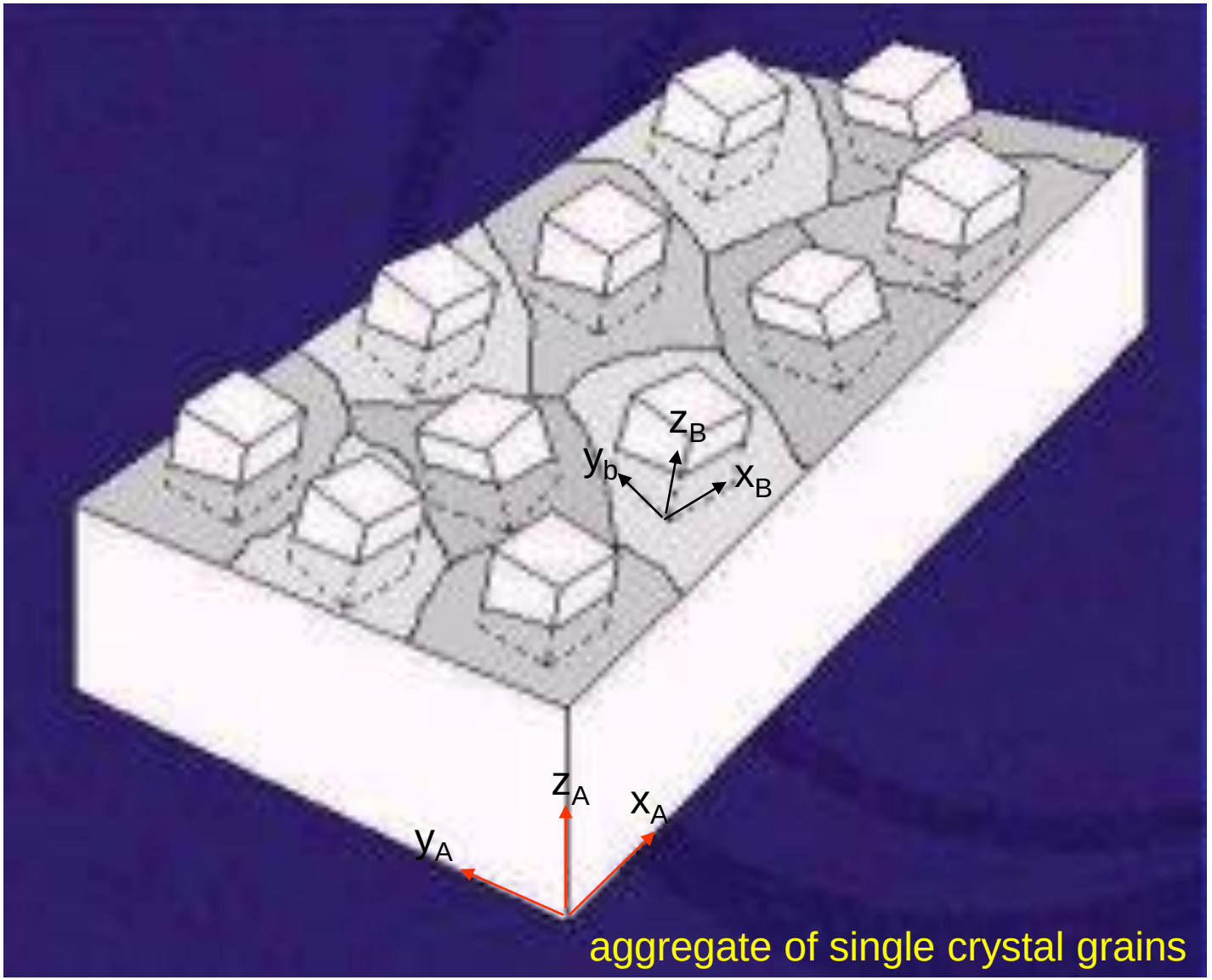

Electron Diffraction Pattern of the Kikuchi type

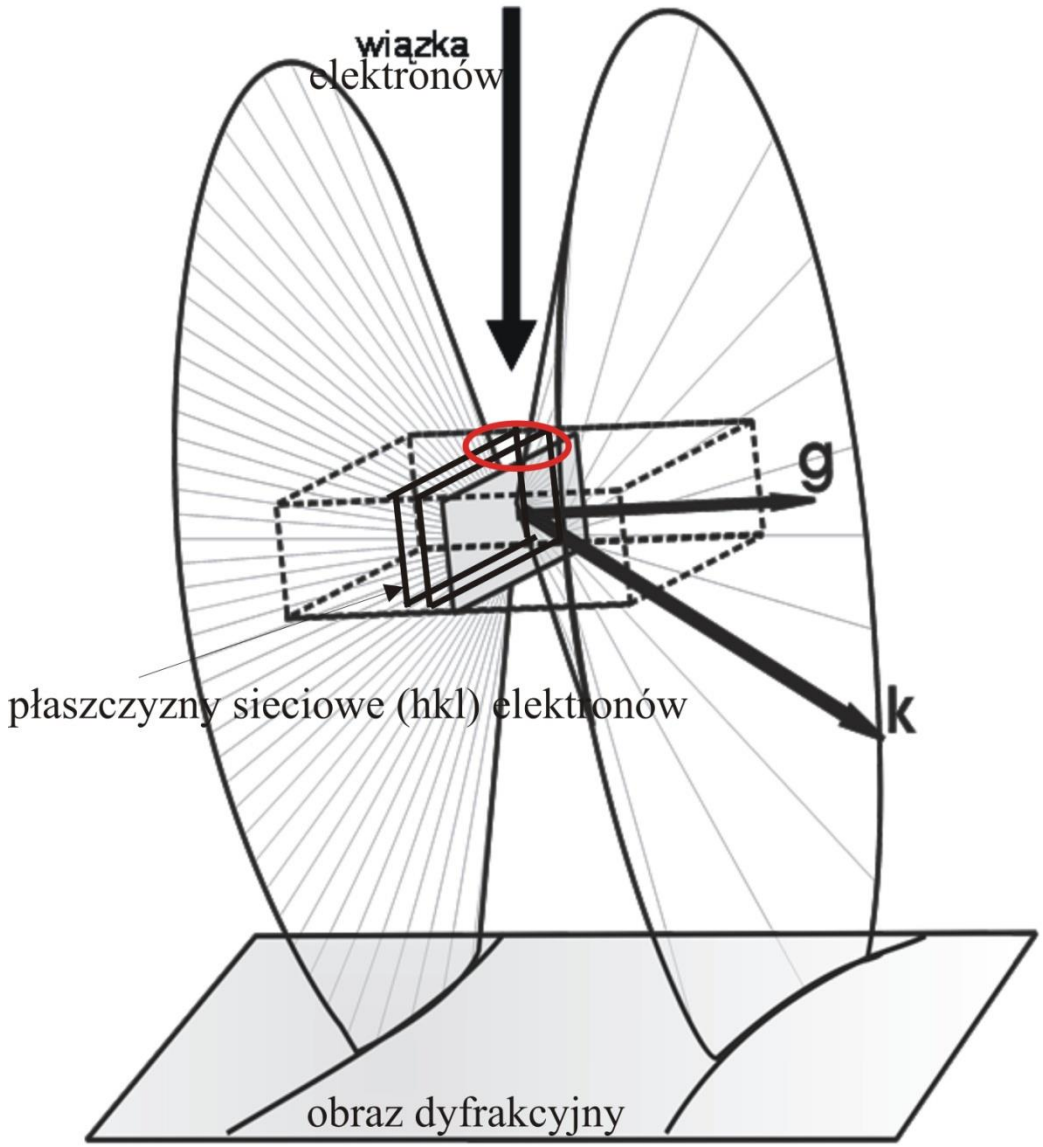

Crystal Orientation Mapping

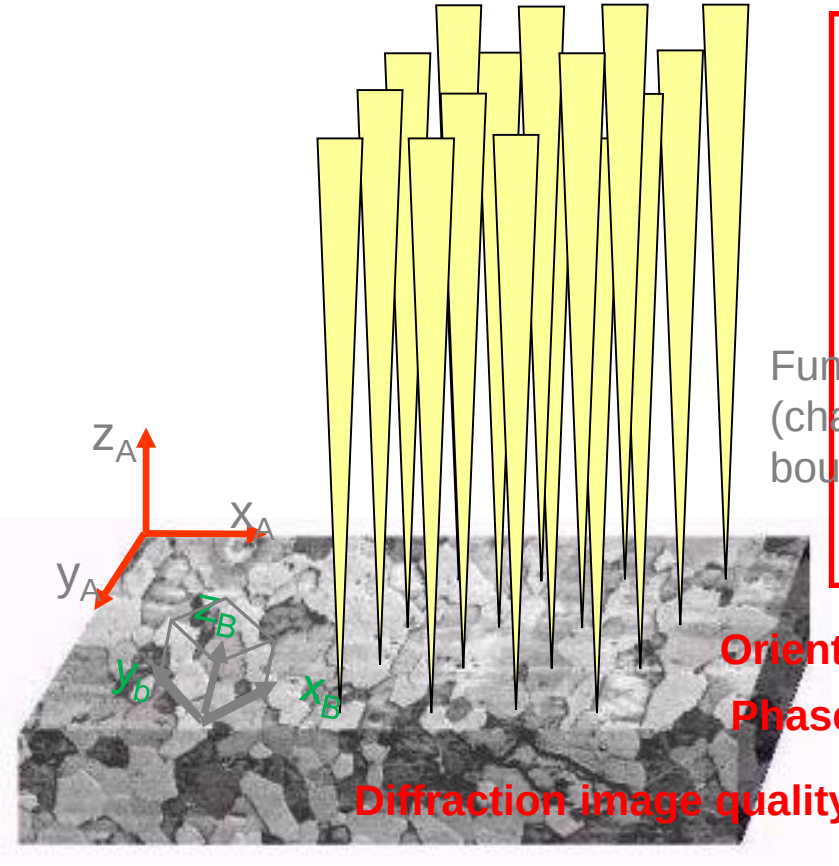

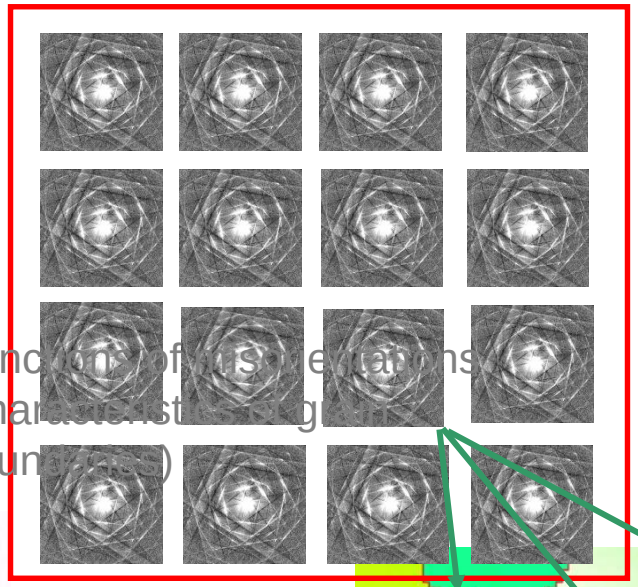

Functions of orientations
(characteristic grain
boundaries)

Orientation

Phase

Diffraction image quality factor

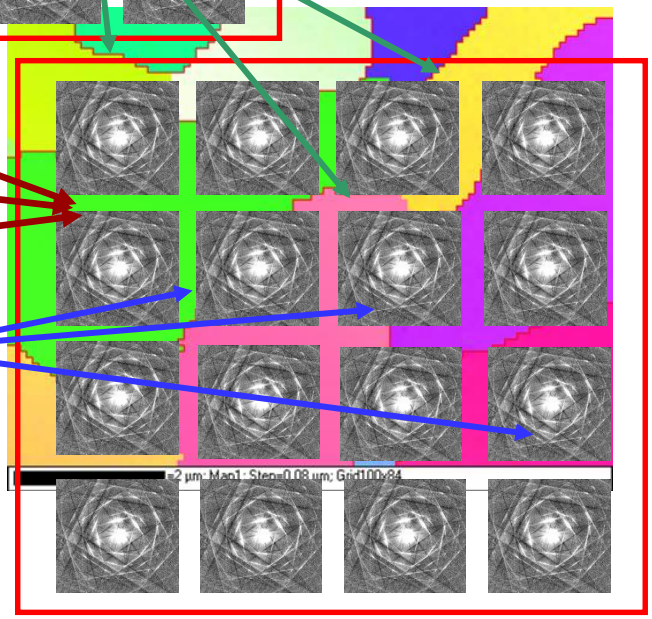

Functions of orientations
(e.g. Texture)

Deformation and strain characterization using Misorientation

Average misorientation map.

Colors are correlated with the mean misorientation angle in grain (100 pairs of orientations are chosen from the grain to calculate mean misorientation for a single grain). This gives information about orientation spread in the grain.

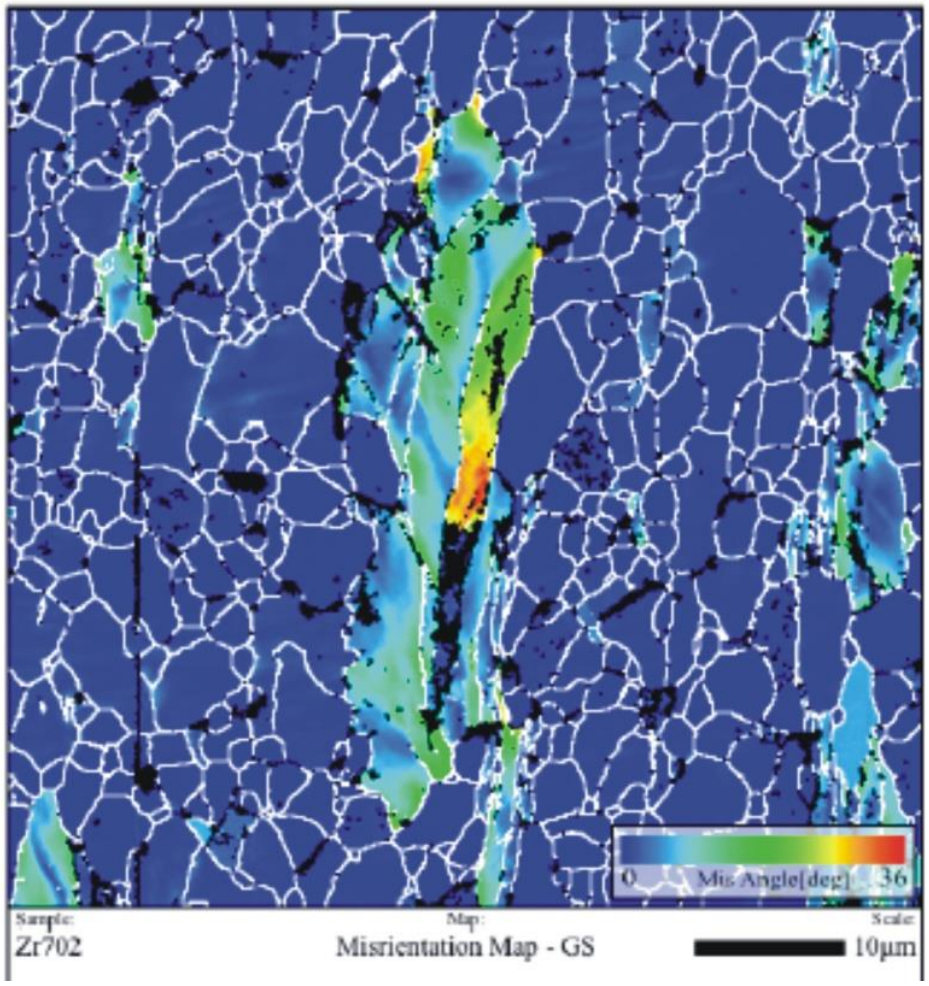

Misorientations are used to visualize local strain variations.

K. Sztwiertnia, G. Sawina: in preparation.

Definition of different types of stresses at various spatial scales

Scale of the first order stresses

(the macrostress σ_{ij}^{M} is the mean value over V_A volume)

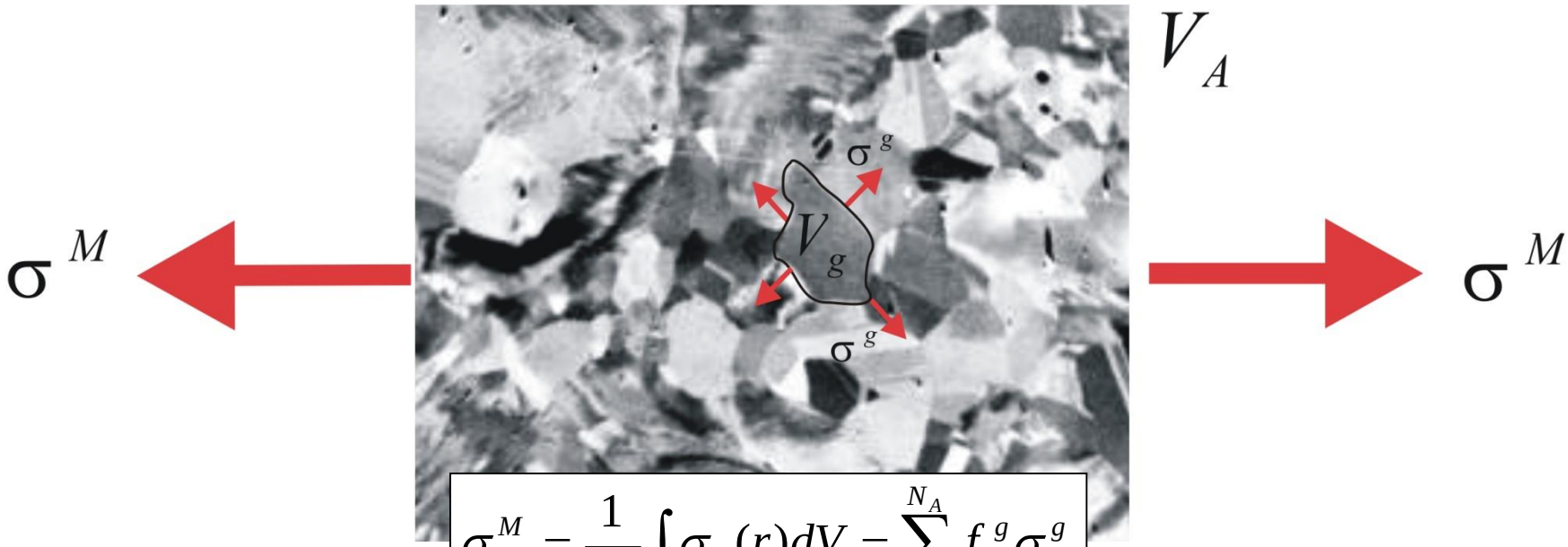

$$\sigma_{ij}^{M} = \frac{1}{V_A}\int_{V_A}\sigma_{ij}(r)dV = \sum_{g}^{N_A} f^{g}\sigma_{ij}^{g}$$

where: N_A - total number of grains $\sigma_{ij}(r)$ - local stress at *r* position

$f^{g} = \frac{V_g}{V_A}$ and σ_{ij}^{g} - the volume fraction and the mean stress for grain *g* having volume V_g

Definition of different types of stresses at various spatial scales

Scale of the second order stresses

(σ_{ij}^{g} is the mean stress for the volume V_g of the g– th grain)

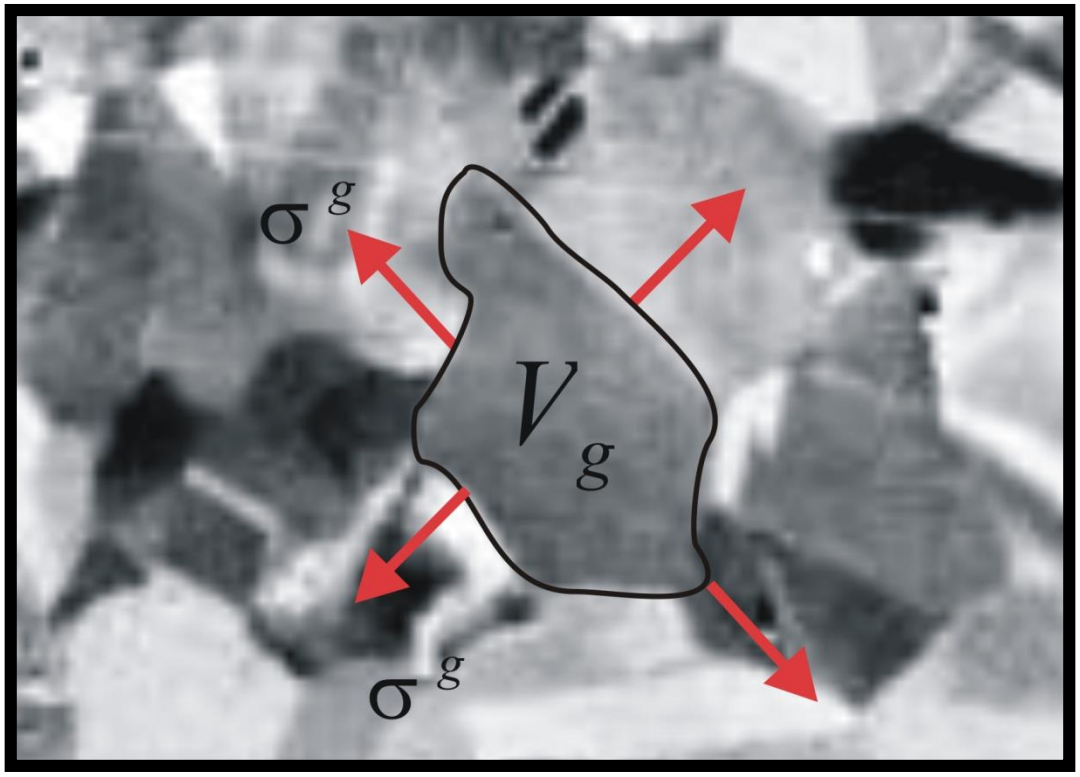

$\sigma_{ij}^{IIg} = \sigma_{ij}^{g} - \sigma_{ij}^{I}$ where $\sigma_{ij}^{I} = \sigma_{ij}^{M}$ for single phase material

Definition of different types of stresses at various spatial scales

Scale of the third order stresses

(the local stress at ***r*** position is indicated)

$$\sigma_{ij}^{III}(r) = \sigma_{ij}(r) - \sigma_{ij}^{g}$$

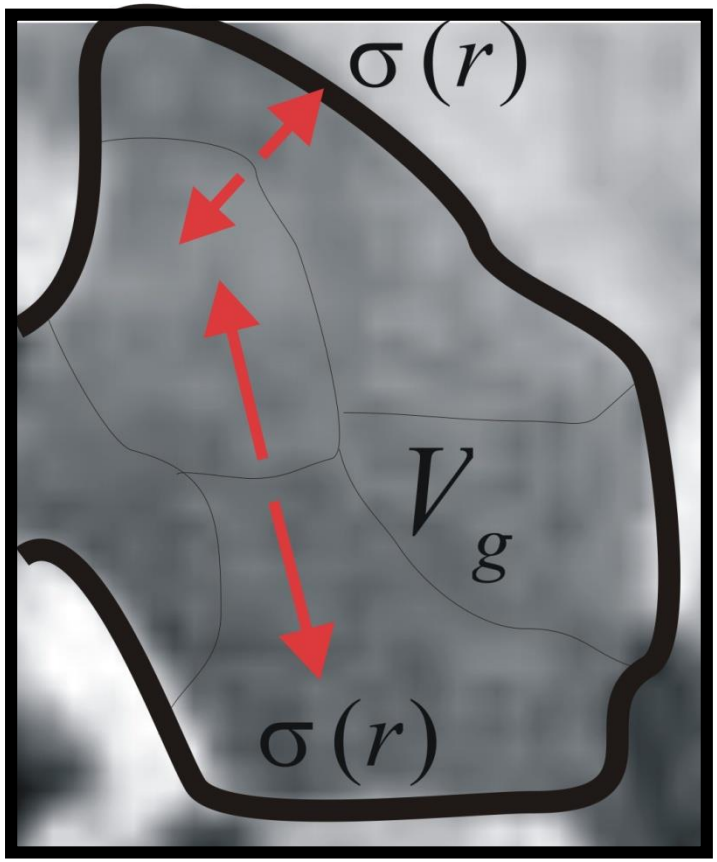

The second order stresses

Residual elastic stresses in the polycrystalline materials affect their properties. For example, the local stress in microelectronic semiconductor devices can lead to defects in the crystal structure and their destruction. Therefore, the study and understanding of the causes of residual stress is important in the operation and prevention of breakdown microelectronic devices. Determination of these stresses is important from the point of view of optimizing the manufacturing process and maintaining the service.

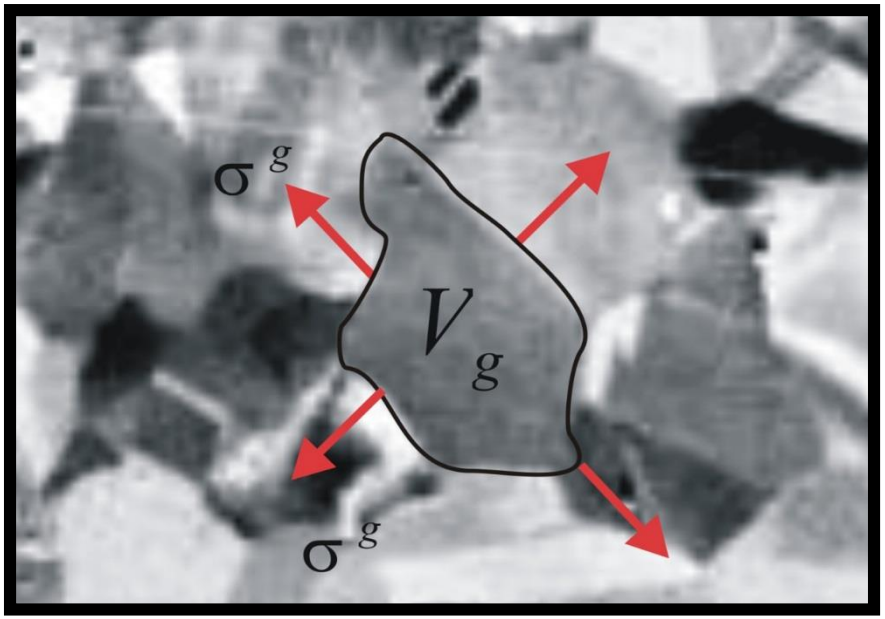

Methods for determining residual stresses:

– X-ray diffraction,
– neutron diffraction,

and eg

– Raman spectroscopy,
– ultrasonic methods,
– EBSD/SEM

and CBED/TEM

Compared with the CBED/TEM - low spatial resolution.

Disadvantage of CBED/TEM – stress relaxation due to thinning of the sample.

A critical analysis of stress measurement by CBED/TEM

•TEM*Strain* is a package for determination of strain with respect to a reference crystal lattice based on convergent beam electron diffraction (CBED) patterns. By computing a complete strain tensor, it provides the actual lattice parameters. Therefore, it can be seen as a tool for determination lattice parameters. Moreover, the package has the capability of determining microscope voltage and camera length.

•The calculations are based on matching experimental and simulated diffraction patterns. In the process the simulated patterns are calculated numerous times. Taking into account long computation times needed for dynamic simulations, the matching relies mainly on kinematic simulations. The package allows for dynamic simulation of CBED patterns but this is an auxiliary feature.

The second order stresses

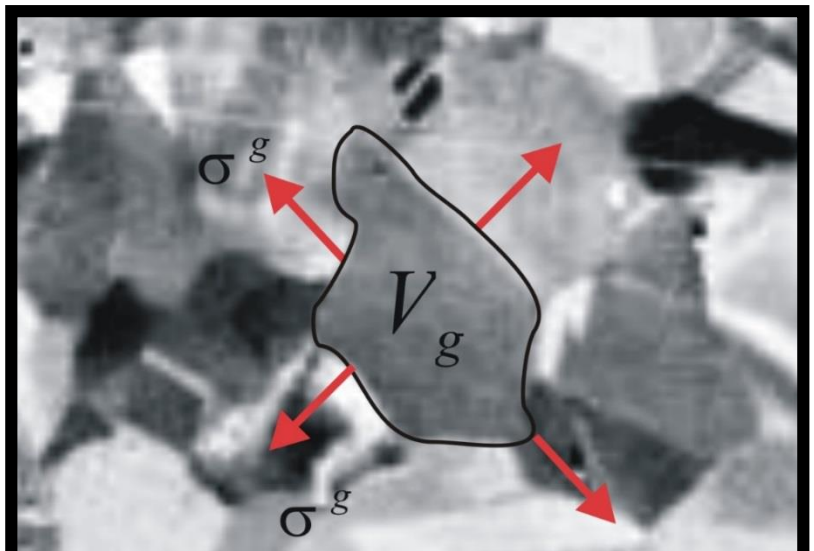

Effect of tensile elastic strain on Kikuchi band width

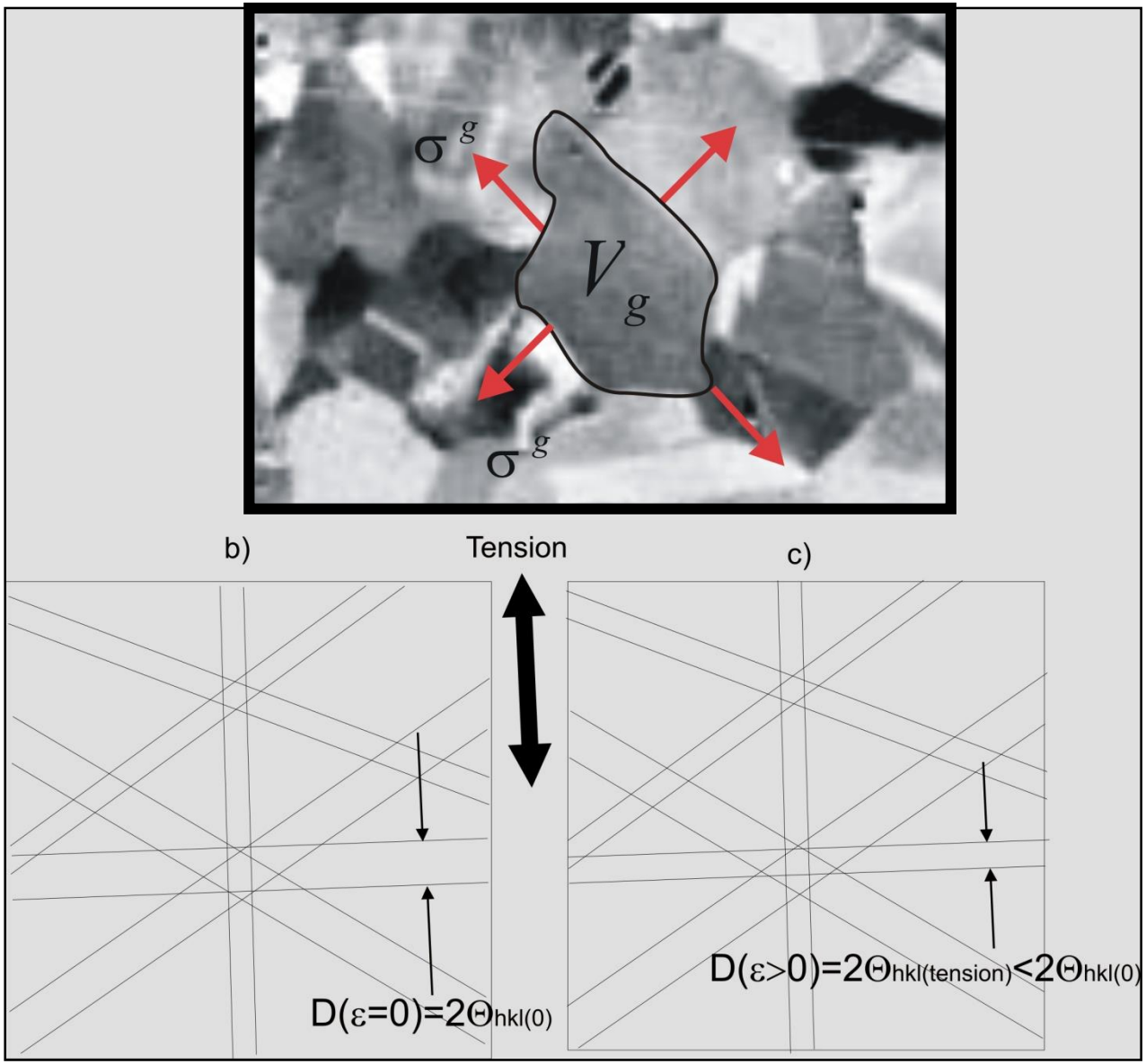

Second order stresses

$$D \approx 2l\theta$$

$$n\lambda = 2d_{hkl} \sin\theta = 2d_{hkl}\theta$$

$$D \approx \frac{2l\lambda}{d} \quad \textit{where: } l - \textit{distance phosphor screen} - \textit{sample}$$

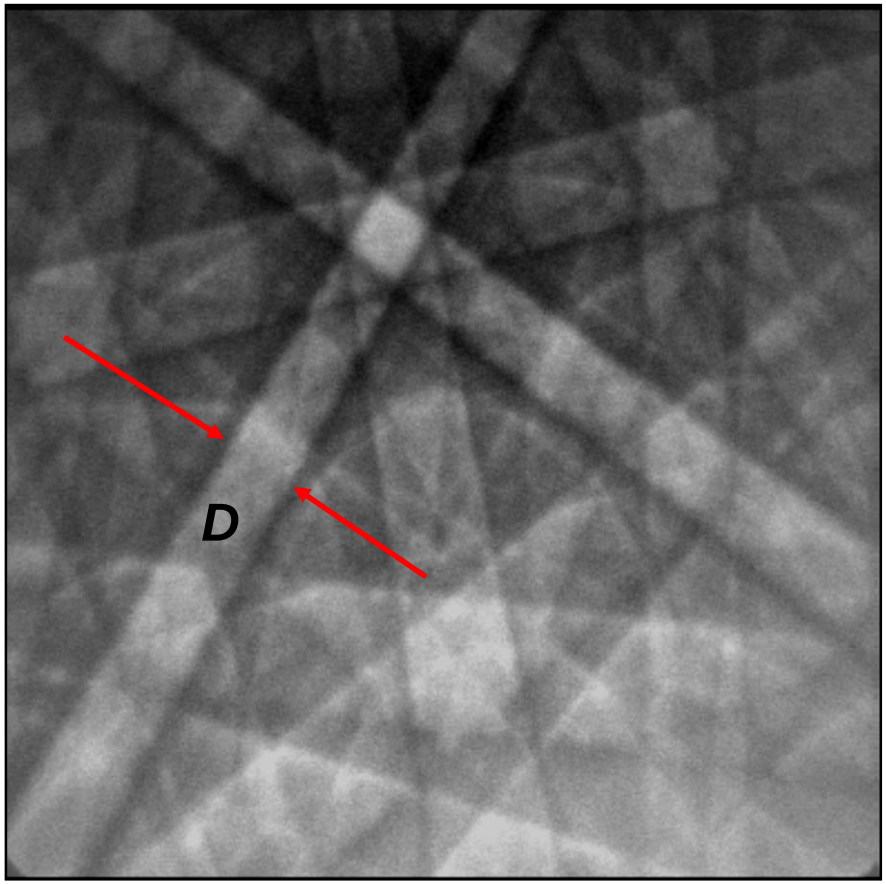

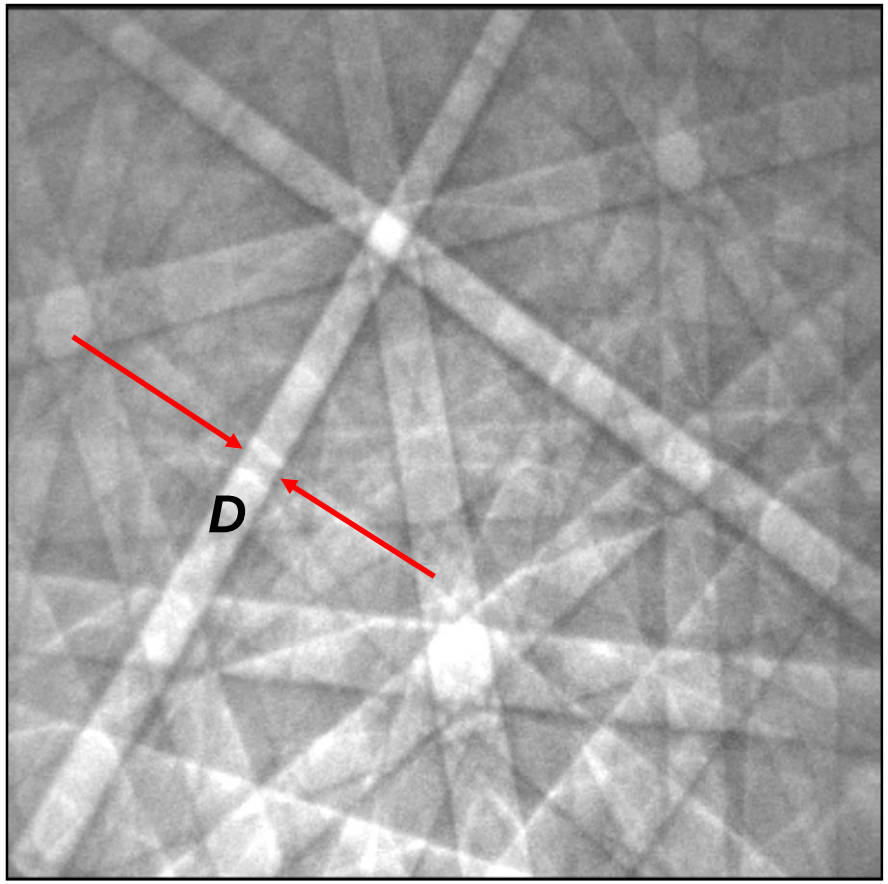

Second order stresses

Question:

which components of strain tensor can be derived unambiguously and which are indeterminate?

Deformation is evaluated by matching the simulated diffraction pattern with the experimental one. Stress tensor is determined from the position of the HOLZ lines (high-order Laue zone).

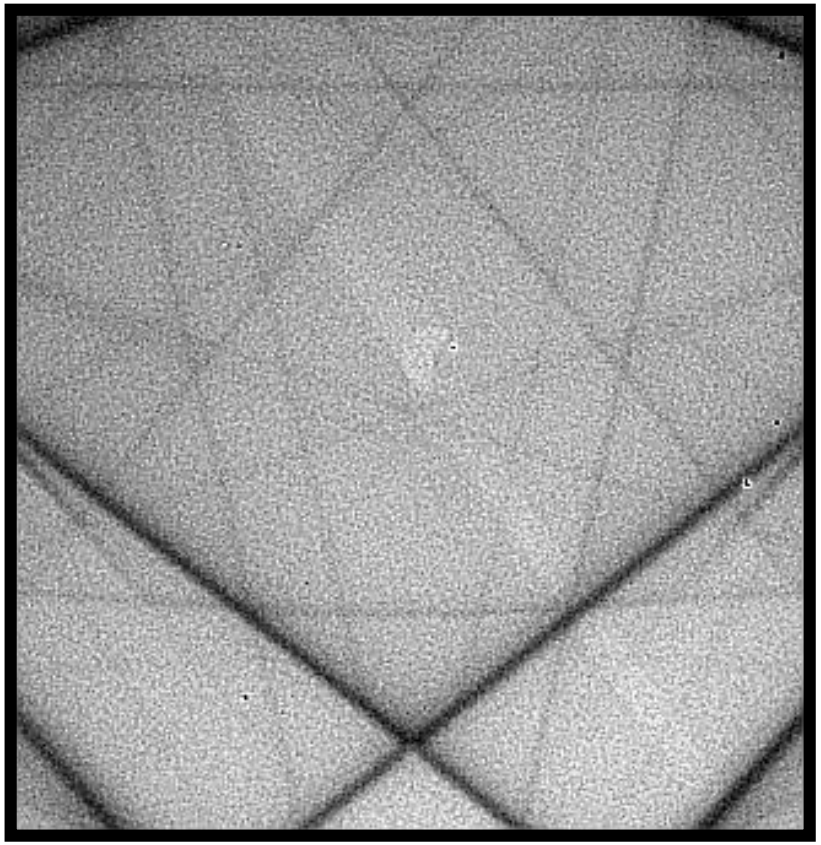

Linie HOLZ

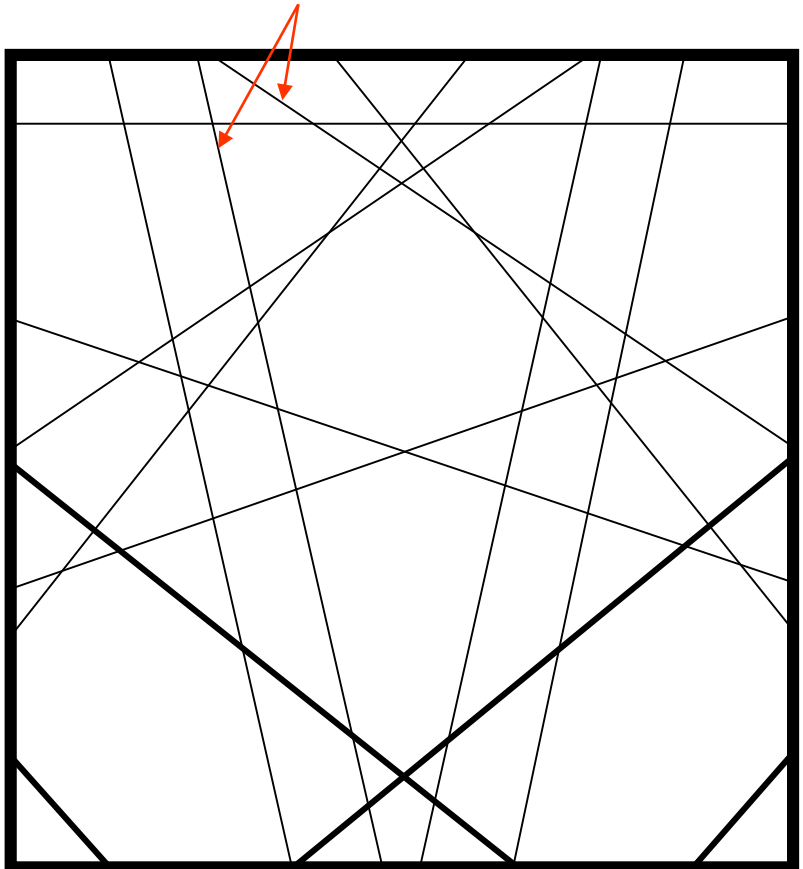

The principle of the evaluation

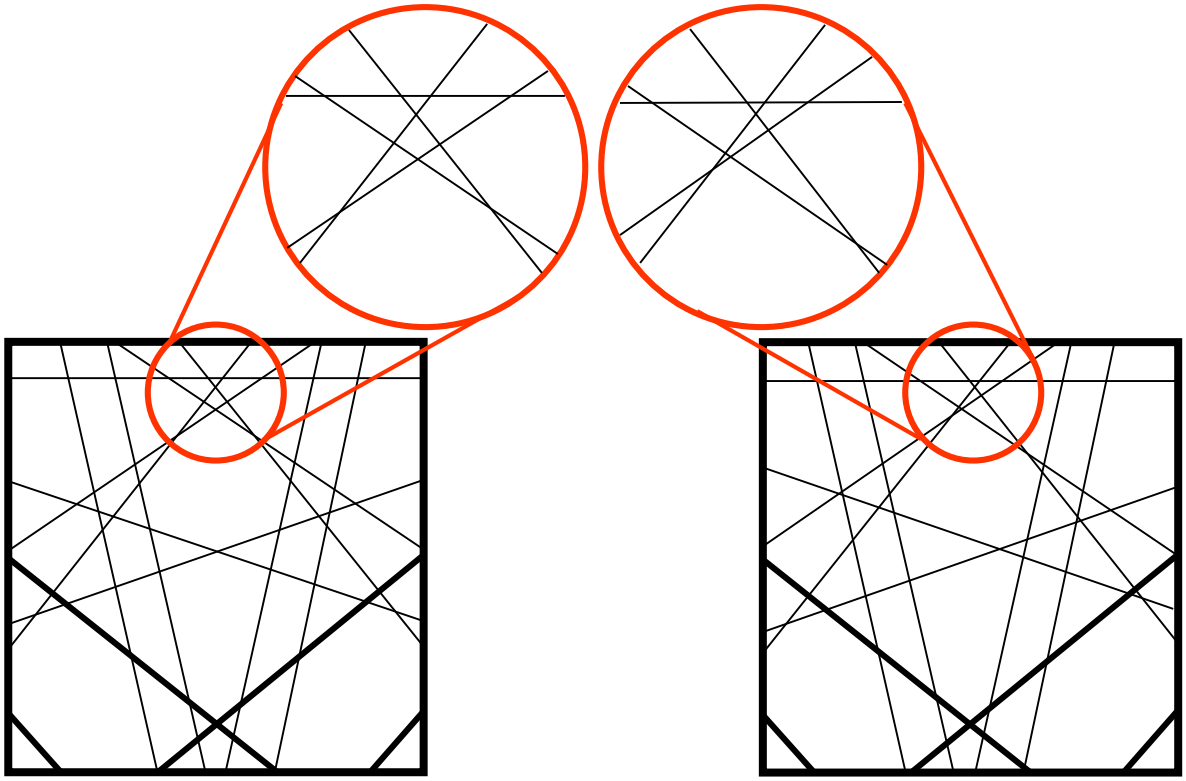

The calculations come down to determine the distance between the intersections of HOLZ lines and express the position of the points of intersection as a function of strain tensor.

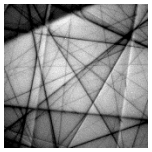

Fitting experimental and simulated patterns

Procedures based on distances between the HOLZ line intersection points.

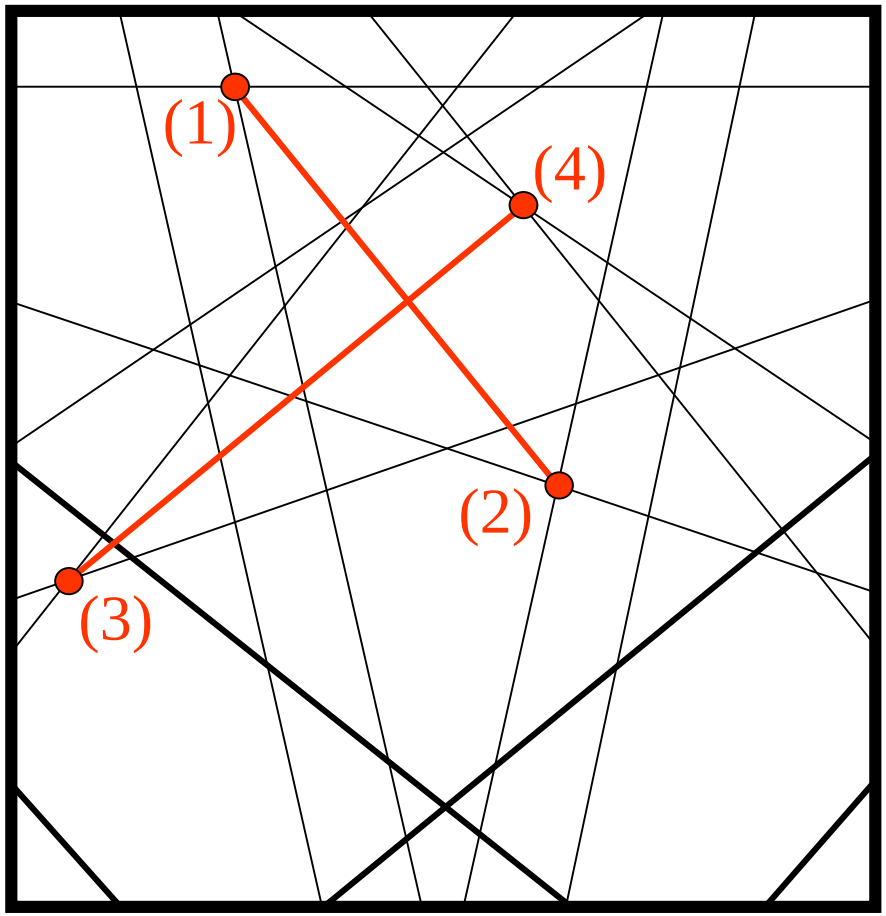

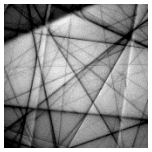

Comparison of experimental and simulated patterns

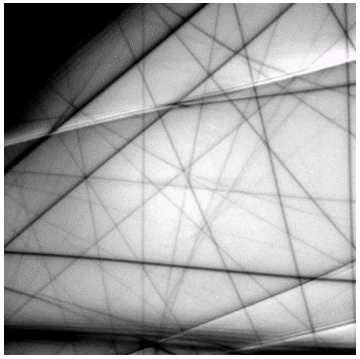
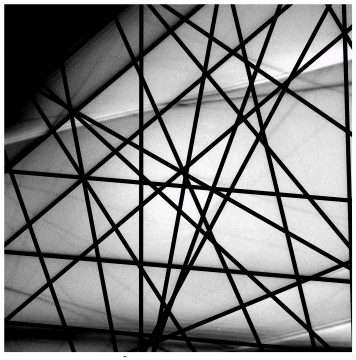
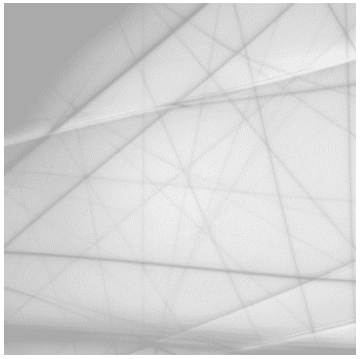

Experimental pattern + Model
Fitting procedure
Result = parameters of the best fit

However,
even a perfect a match ***does not*** guarantee
correctness of the results.

Due to the ambiguity problem (the same pattern can be simulated with different lattice parameters) it is more convenient to see the TEMStrain as a determination of small deviations from reference lattice parameters.

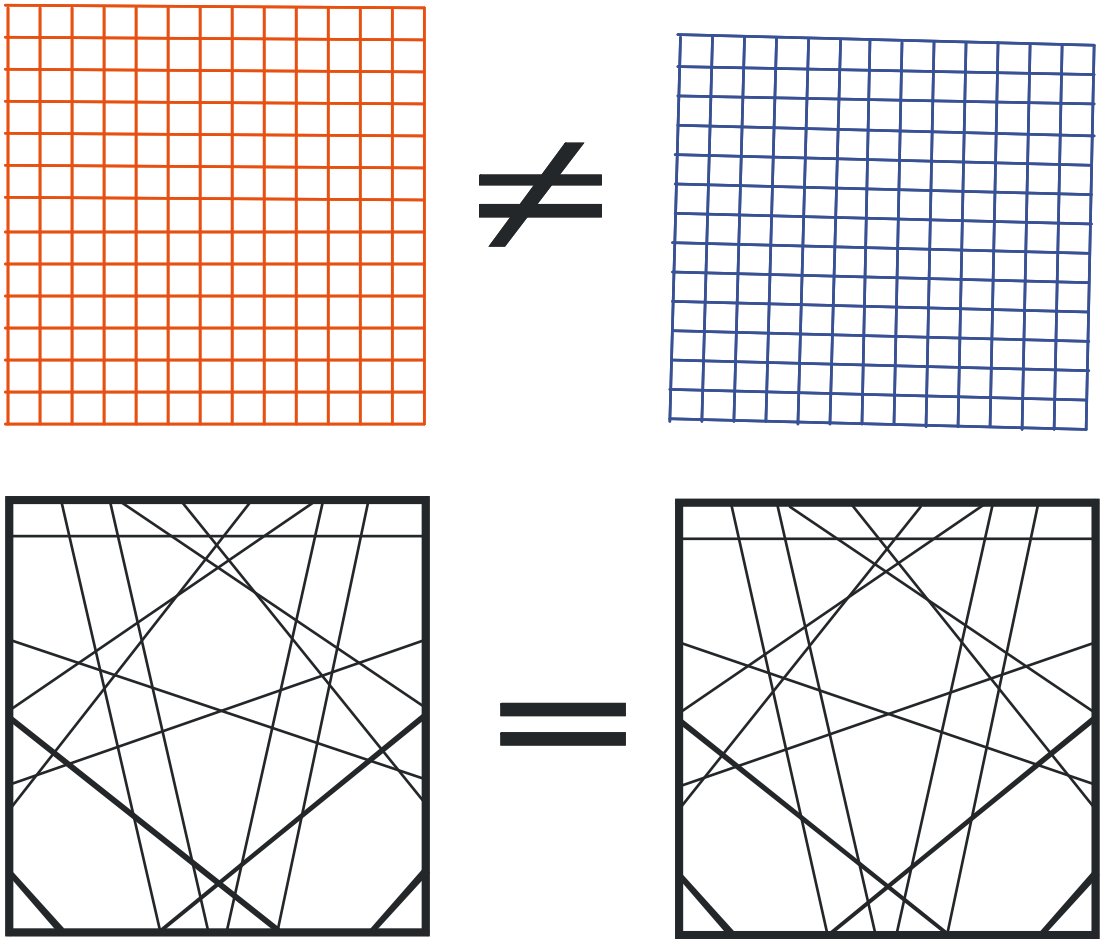

Maier at al. (Phil. Mag. A **74**, 23-43, 1996) : "**most CBED patterns can be simulated by a number of different lattice parameters"**

A. Morawiec - Program: TemStrain

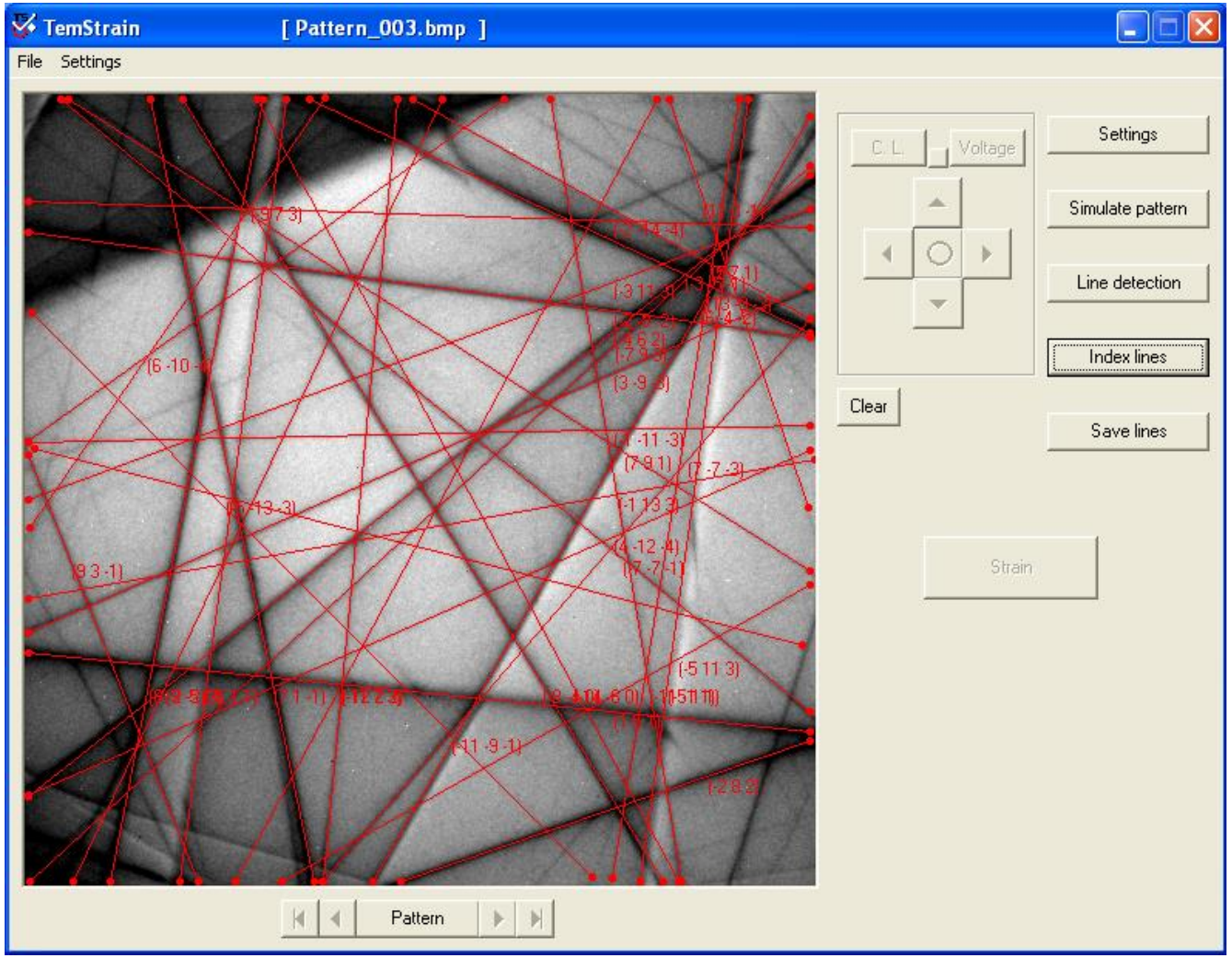

Effect of elastic strain gradient on Kikuchi line width.

(The broadening of original sharpness of diffraction line is connected with the local strain (stress) associated with the local increasing of lattice defects concentration)

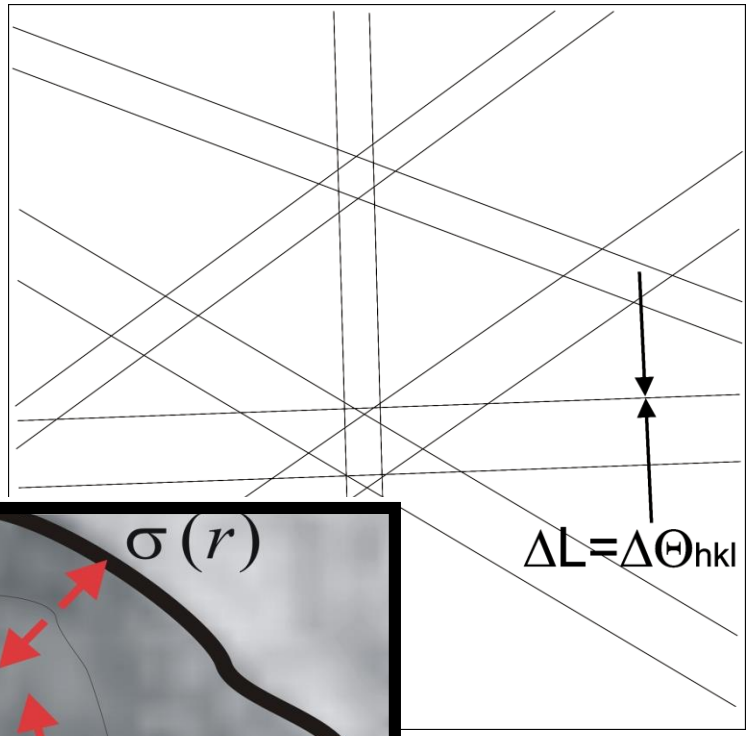

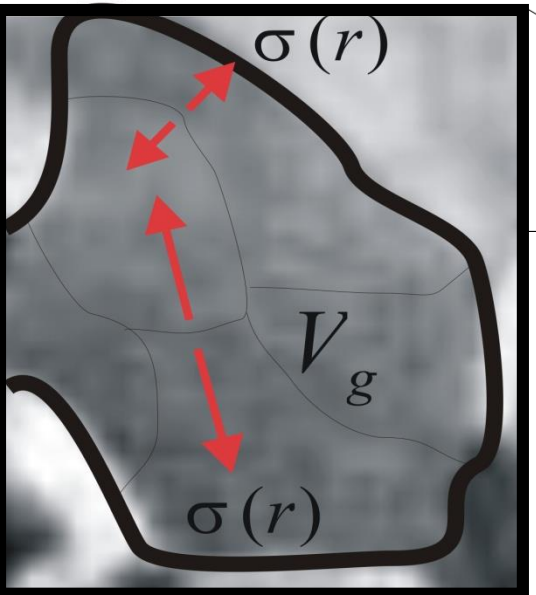

Third order stresses

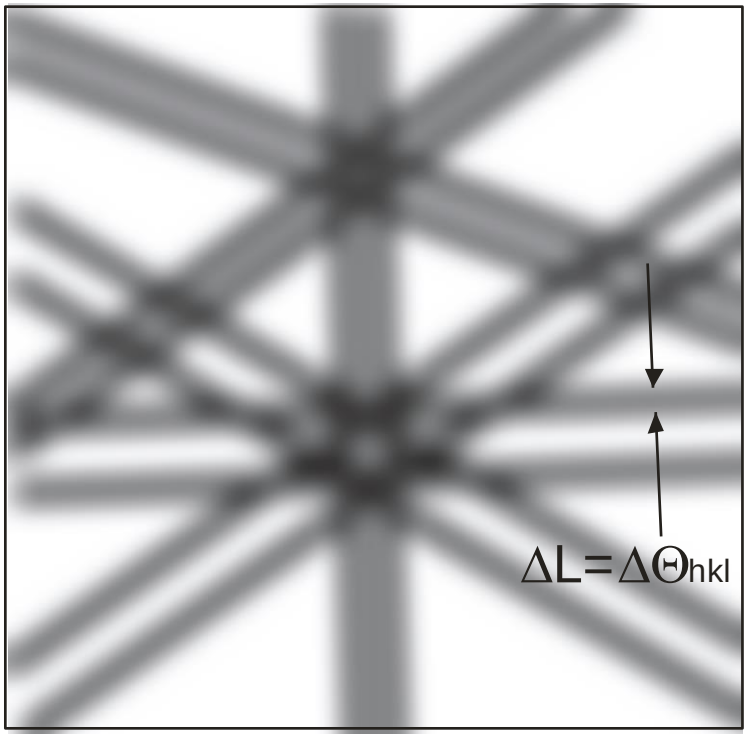

The originally sharp line edge associated with a single d-spacing broadens as numerous spacings contribute to the band.

At first approximation the width of diffraction line correlated with deformation of crystallographic lattice is proportional to the mean value of strain $<\varepsilon>$ or mean value of stress $<\sigma>$.

It is assumed that the broadening of diffraction line is proportional to $\sqrt{\rho_d}$
where: ρ_d - dislocation density.

Band Detection

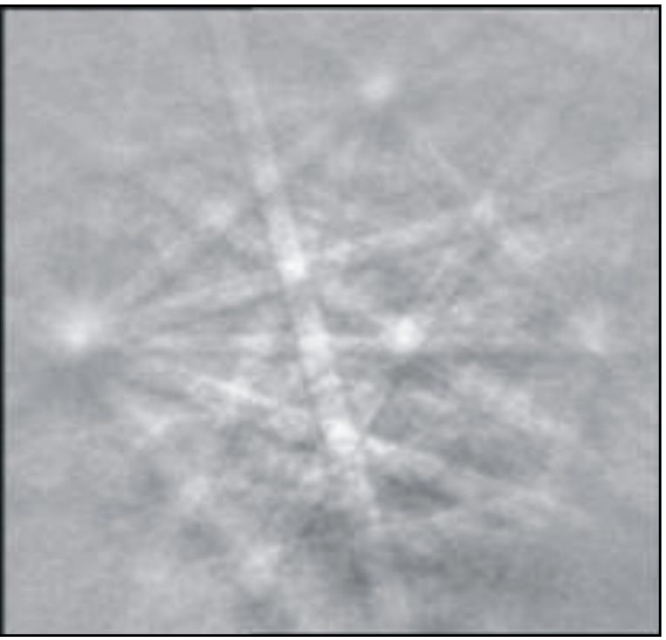

What happens when the line of Kikuchi band is broading

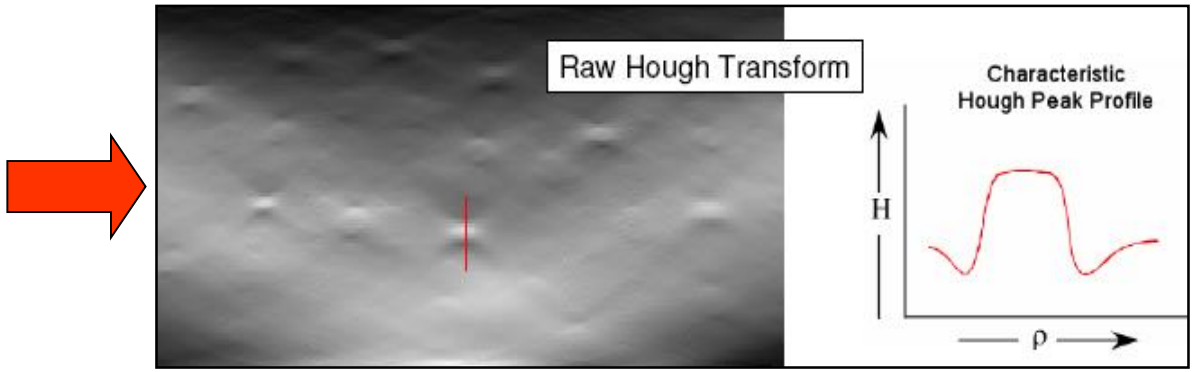

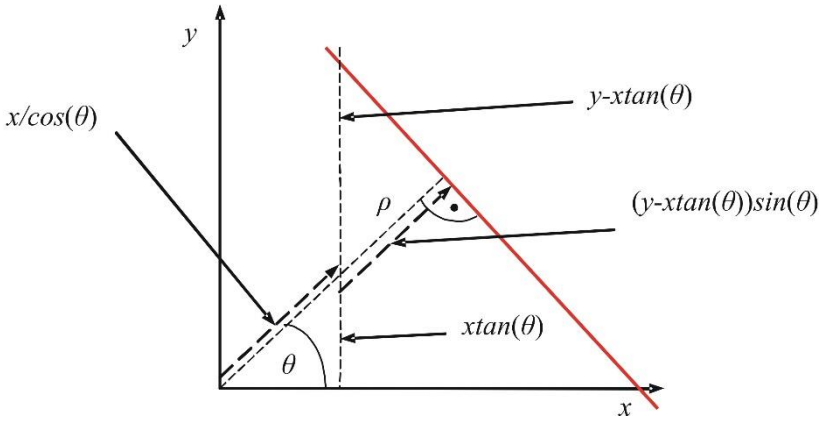

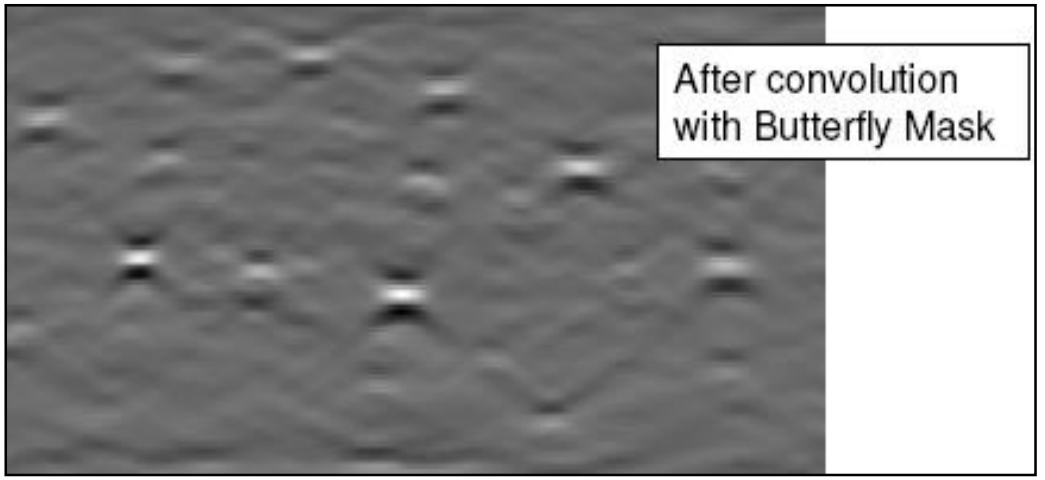

Exemplary cross-section (along ρ) of diffraction lines taken from the region of low strain (low density of crystallographic defects) **(a)** and from the region of high strain (high density of crystallographic defects) **(b)**

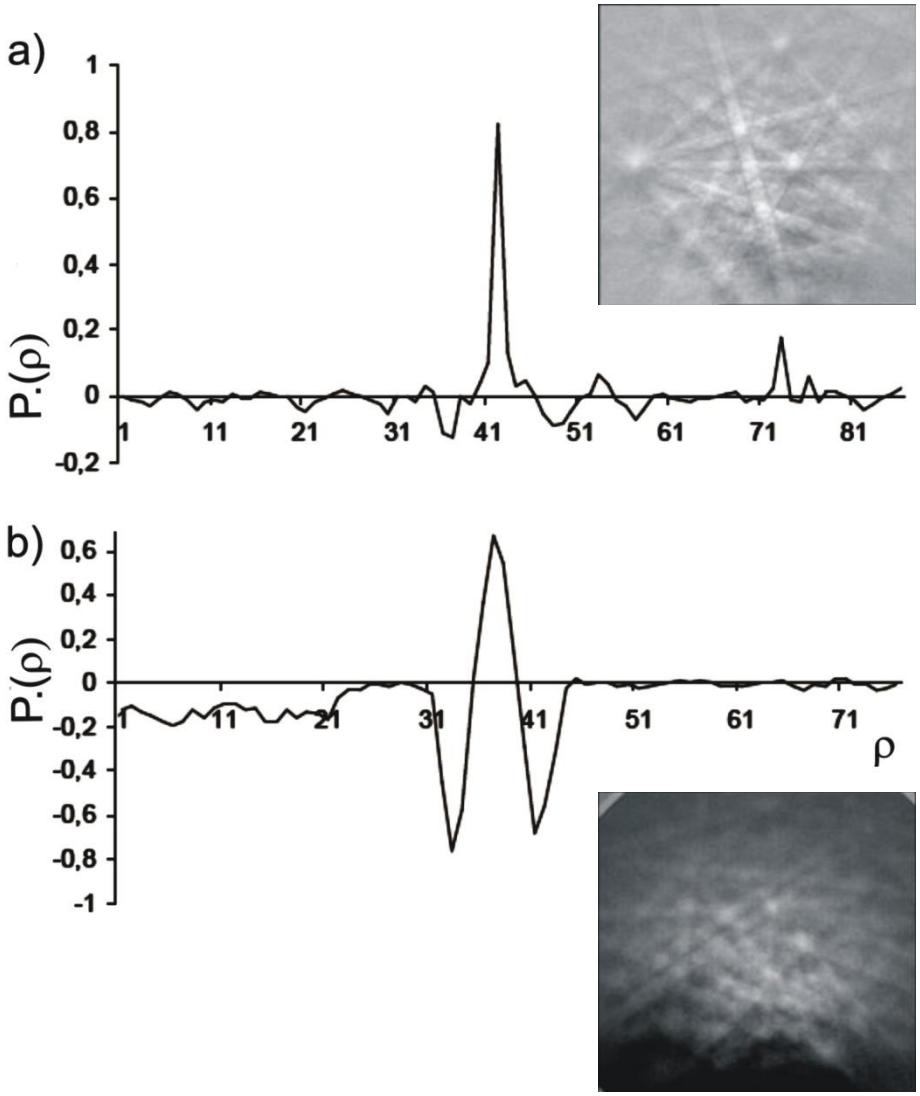

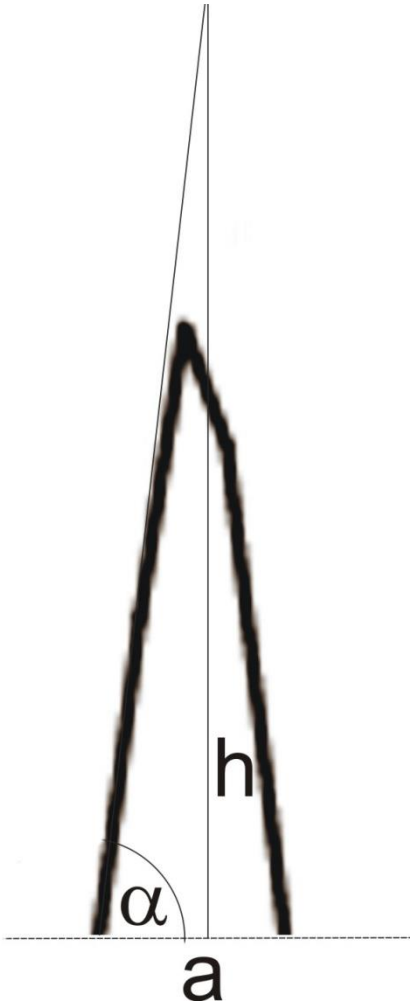

$$P'(\rho) = tg\alpha = \frac{2h}{a} = BS$$

Band Slope parameter is calculated in the following way:

1. **From the Hough space (created for each diffraction) several randomly selected points representing most intensive Kikuchi bands are chosen.**
2. **For each line a directional derivative P’(ρ) is calculated; the average of 7 lines from diffraction pattern is taken as a measure of the broadening.**
3. **Band Slope is estimated at every point of the measure grid.**

Quality index q

$$q = A / BS$$

where: A – constant

BS – Band Slope

Deformation and strain characterization using EBSD Image Quality Factors

Maps showing orientation topography and distribution of local strain in the Cu sample deformed by tension

A. Baczmański, K. Sztwiertnia, M. Faryna: in preparation

Orientation map

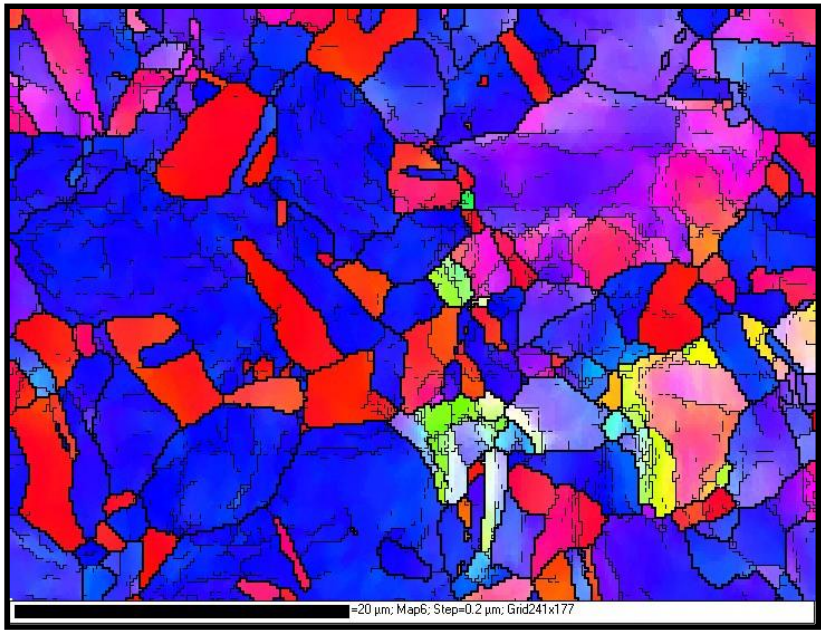

Distribution of local strain based on Band Slope

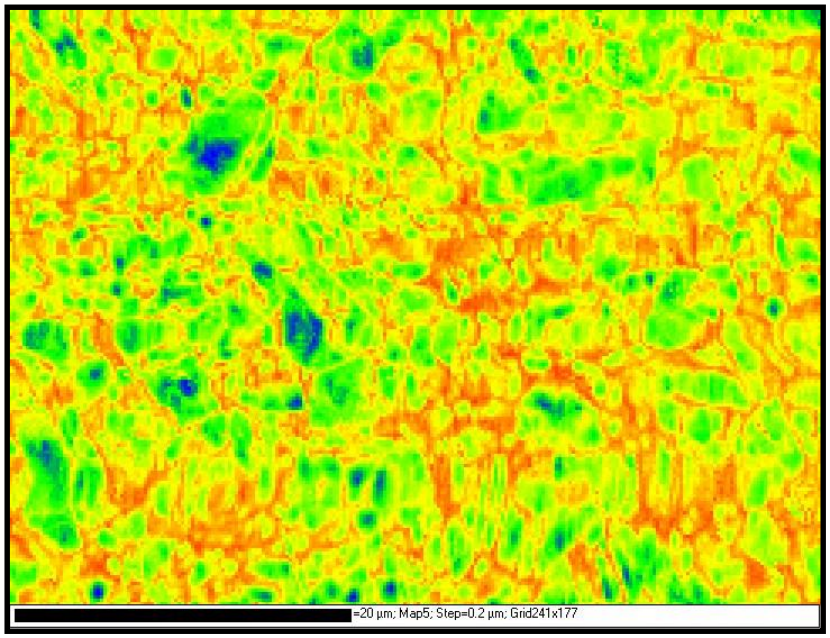

Blue grains are more strained than the red ones.

EBSD measurements of surface local strains in alumina ceramic before shot peening (test sample).

Color scale

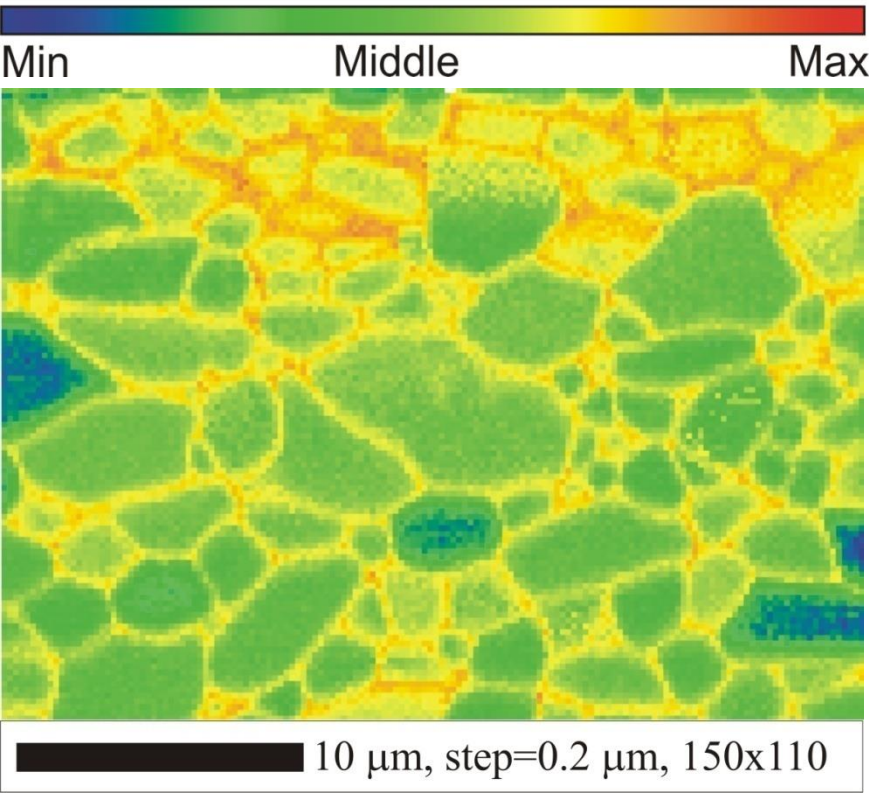

coarse-grained ceramic

q map.

Orientation map; grain boundaries with disorientation angle 20 – 40° → blue, 40 – 60° → black, 60 – 80° → yellow, > 80° →

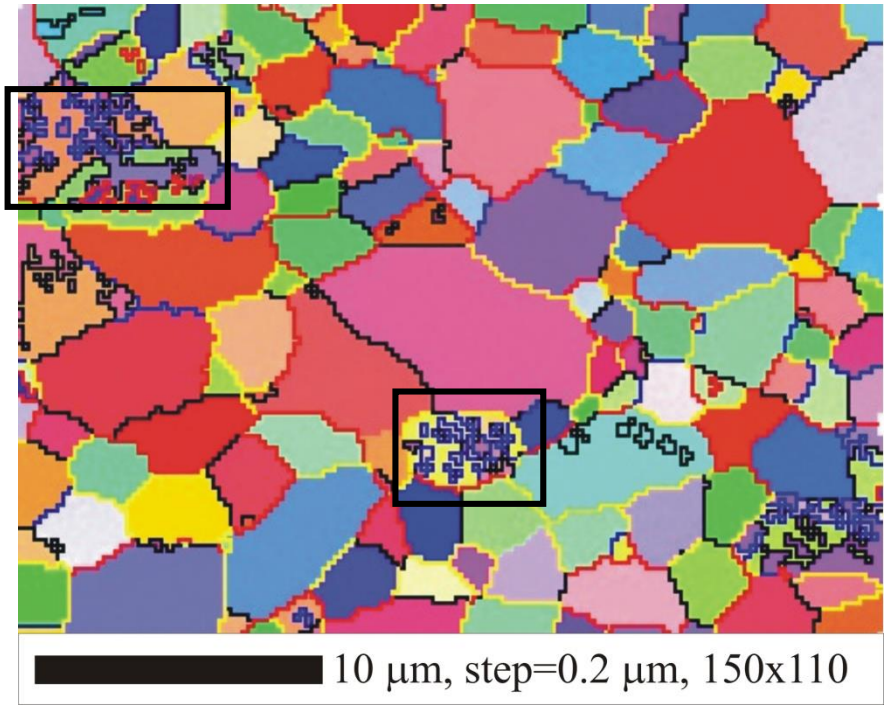

EBSD measurements of surface local strains in Al_2O_3 ceramic before shot peening

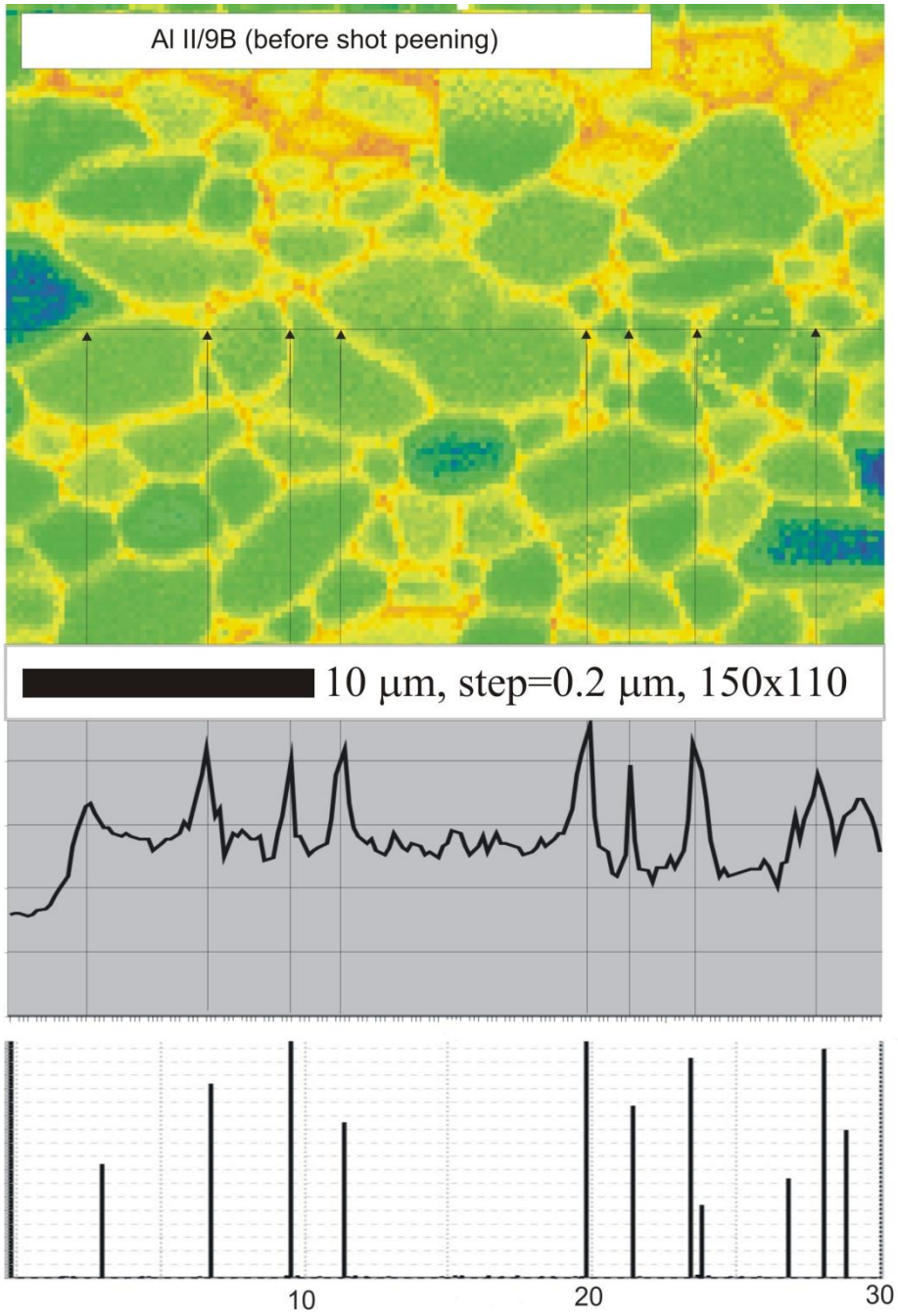

Map of Quality index (q)

Changes of Quality index (q) along the A-A line

Changes of misorientation angle along the A-A line

EBSD measurements of surface local strains in alumina ceramic after shot peening

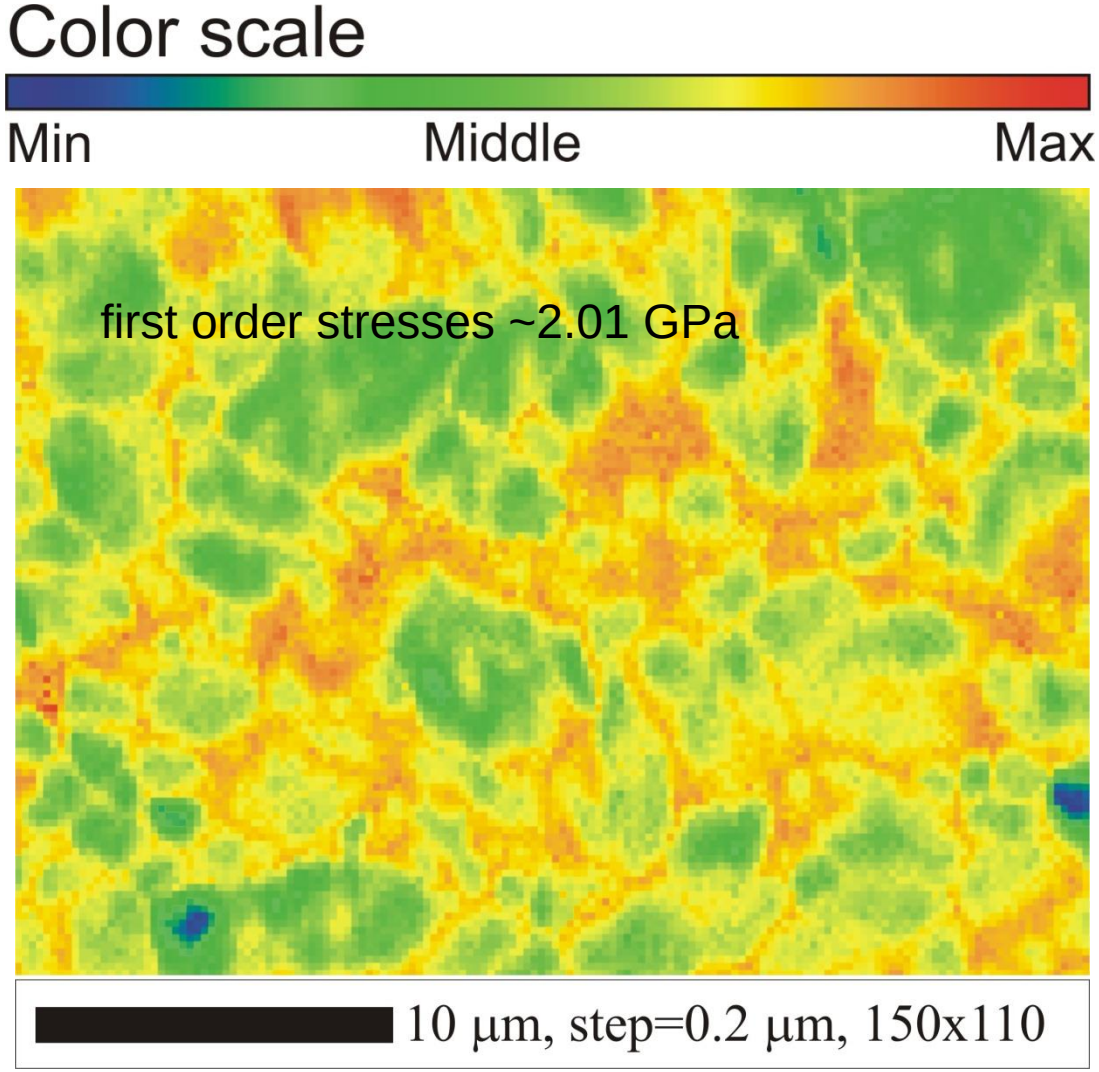

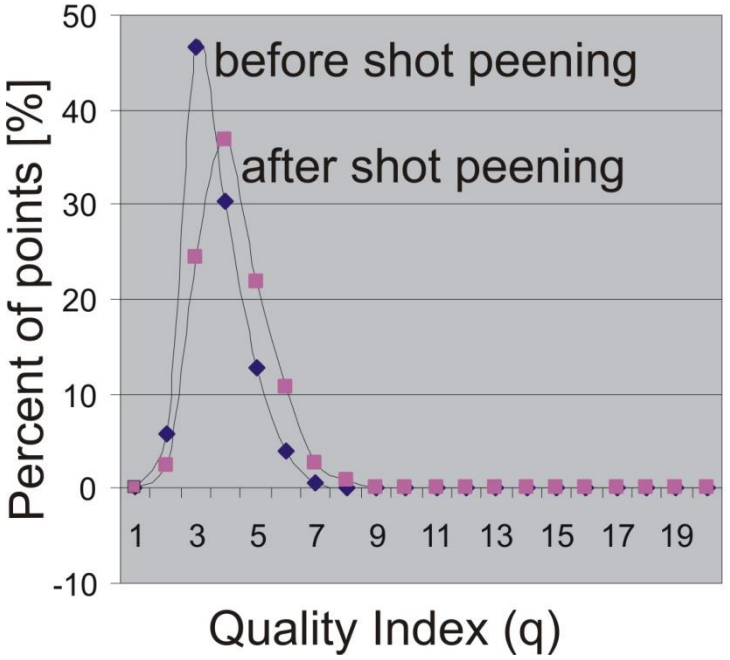

Comparison of normalized q distributions for alumina sample surfaces before and after shot peening.

EBSD measurements of surface local strains in alumina ceramic after shot peening

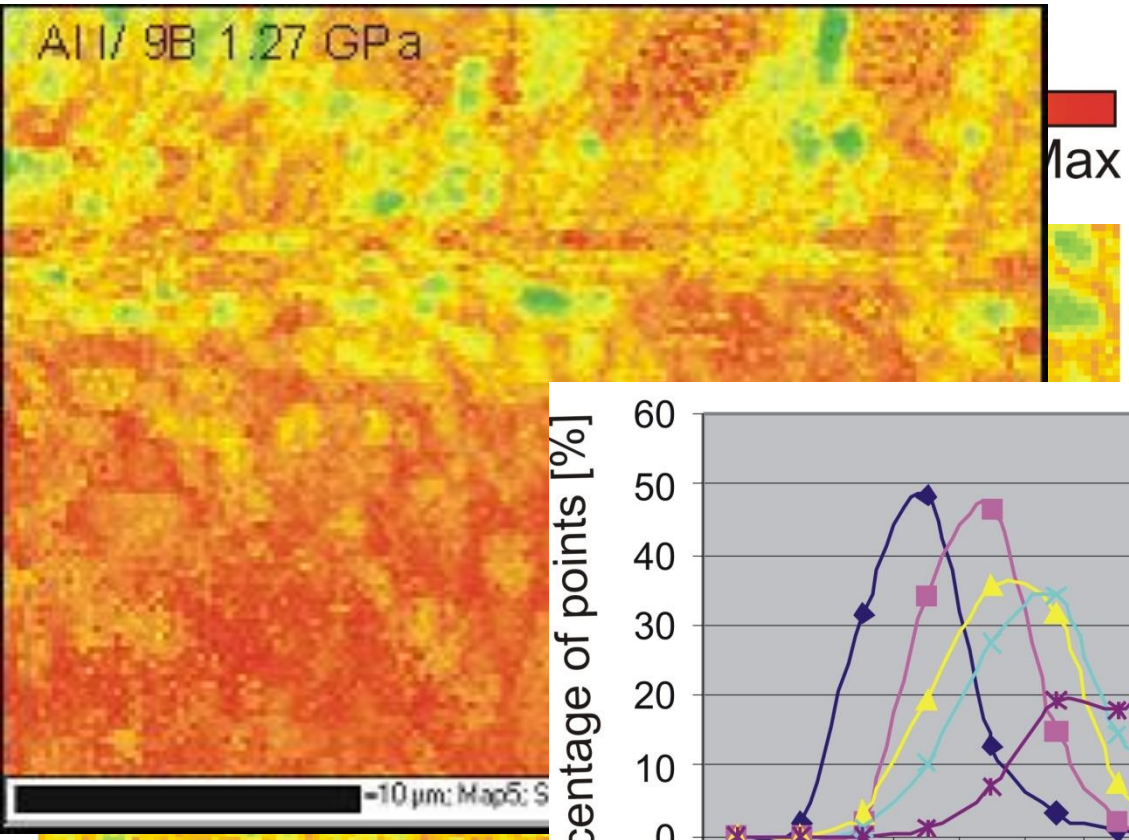

fine-grained ceramic

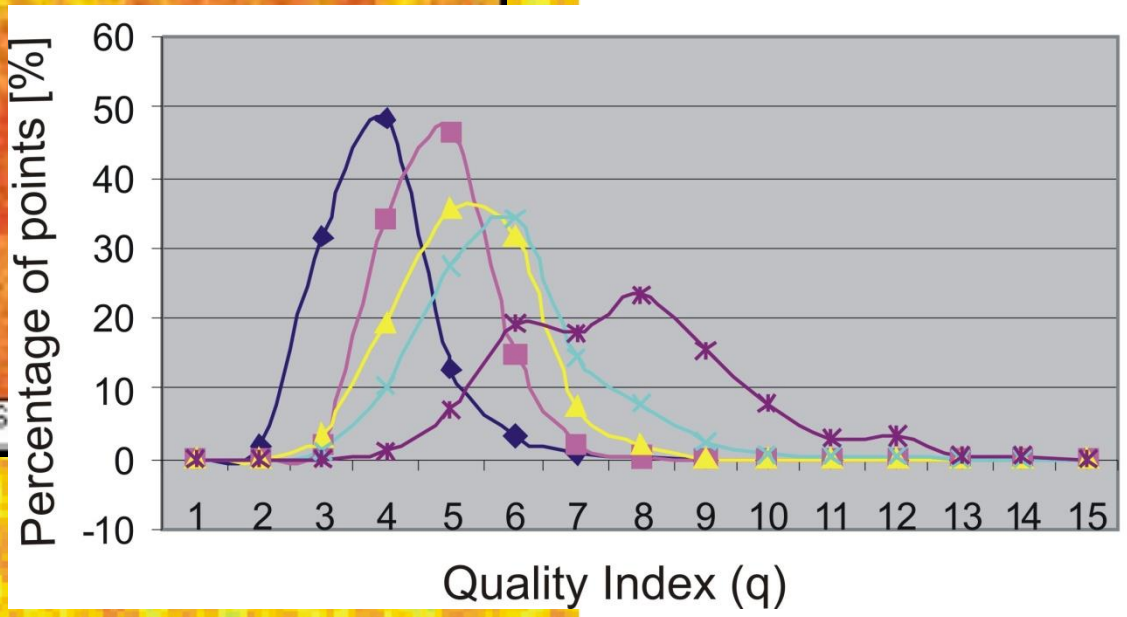

Comparison of normalized q distributions for alumina sample surfaces before and after shot peening: 1 – the test sample, 2 - (first order stresses ~0.35 GPa), 3 - (first order stresses ~0.83 GPa), 4 and 5 - (first order stresses 1.27 GPa).

EBSD measurements of surface local strains in ZrO_2 ceramics before shot peening (test sample)

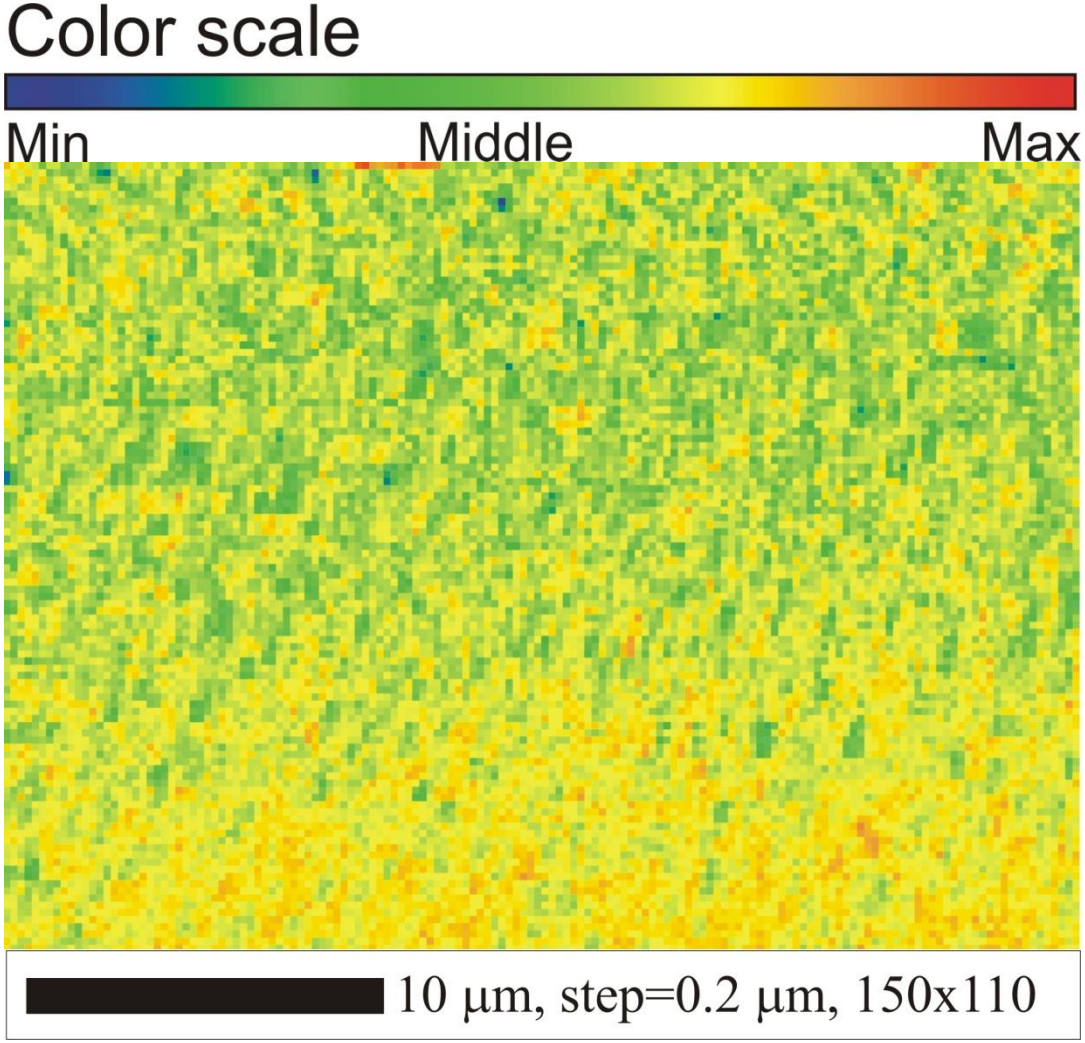

Map of Quality index (q)

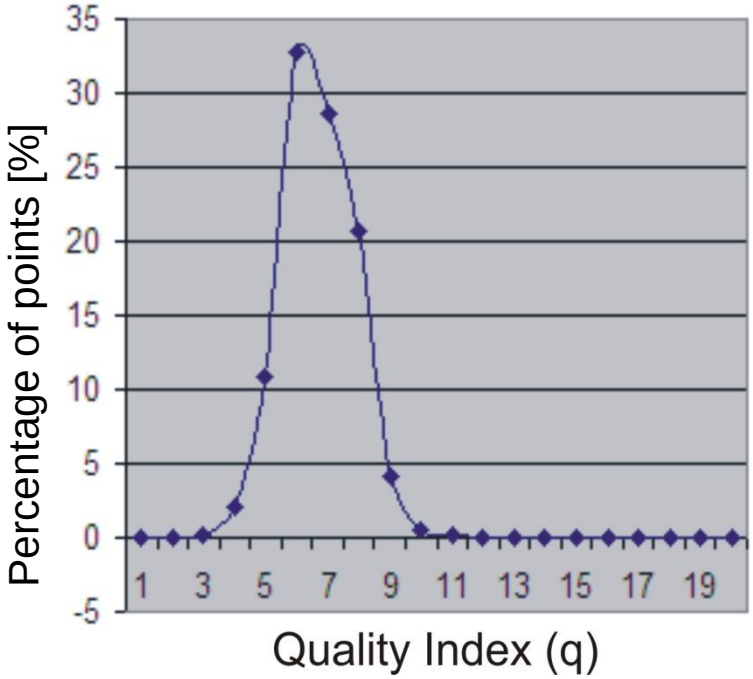

Normalized Quality index (q) distribution surface of ZrO_2 sample before shot peening

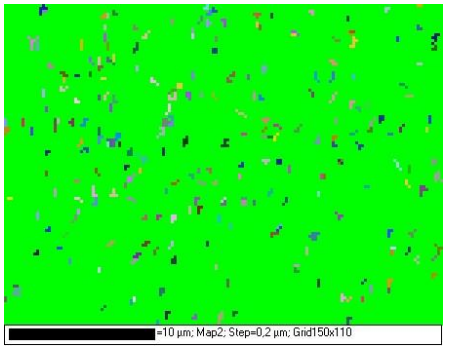

Orientation map

EBSD measurements of surface local strains in ZrO_2 ceramics after shot peening

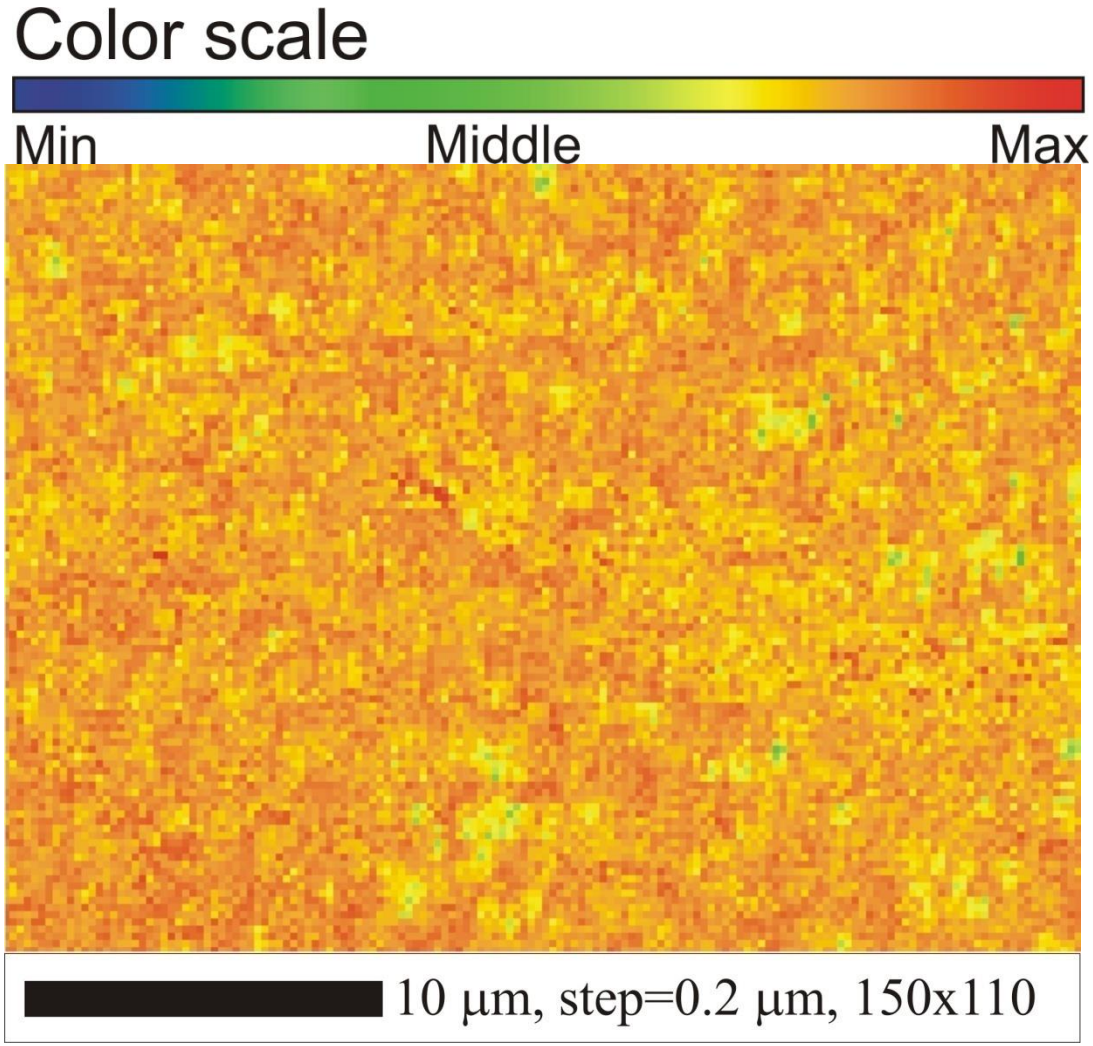

Map of Quality index (q)

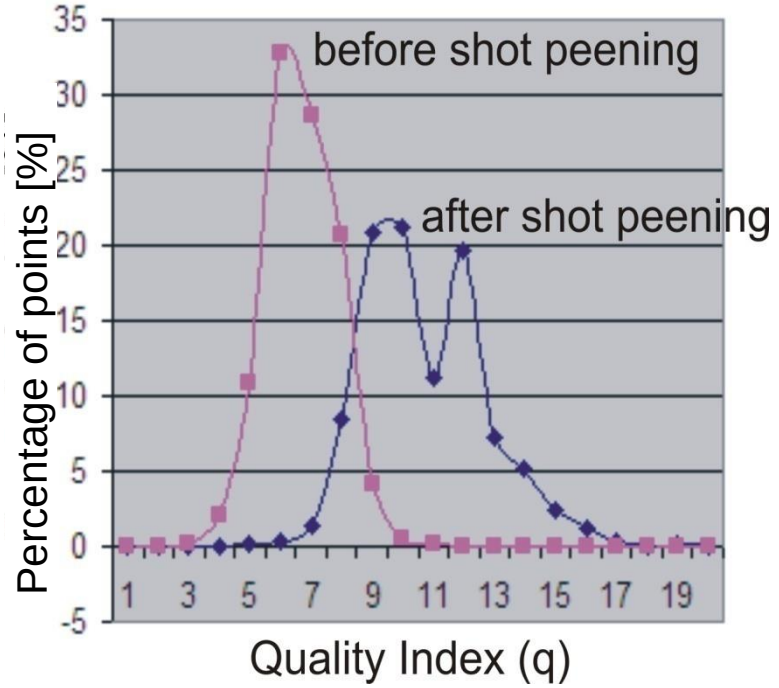

Normalized Quality index (q) distribution surface of ZrO_2 sample after shot peening

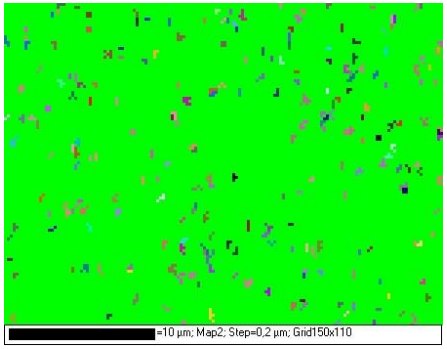

Orientation map

Conclusions

1. **Electron BackScatter Diffraction was successfully applied to detect and map strain fields in subsurface layers of ZrO_2 and Al_2O_3 ceramics before and after shot peening.**

2. **EBSD Quality index *(q)* calculated based on Band Slope value was used as a local strain sensitive parameter to qualify the local distortion of crystallographic lattice.**

3. **Such a measurement is independent from the fact whether the pattern is solved or not (crystallographic orientation is established or not).**

4. **This is a great advantage of such a measurement as the ability of solving the Kikuchi diffraction by standard software in the samples with deformed subsurface layers is very limited due to strong broadening of the bands.**

5. **Analysis of Quality index *(q)* showed that the subsurface layers in the ZrO_2 samples were more deformed compared with the Al_2O_3 ones.**

MICROSTRUCTURE OF POLYCRYSTALLINE ZINC SUBJECTED TO PLASTIC DEFORMATION BY COMPLEX LOADING

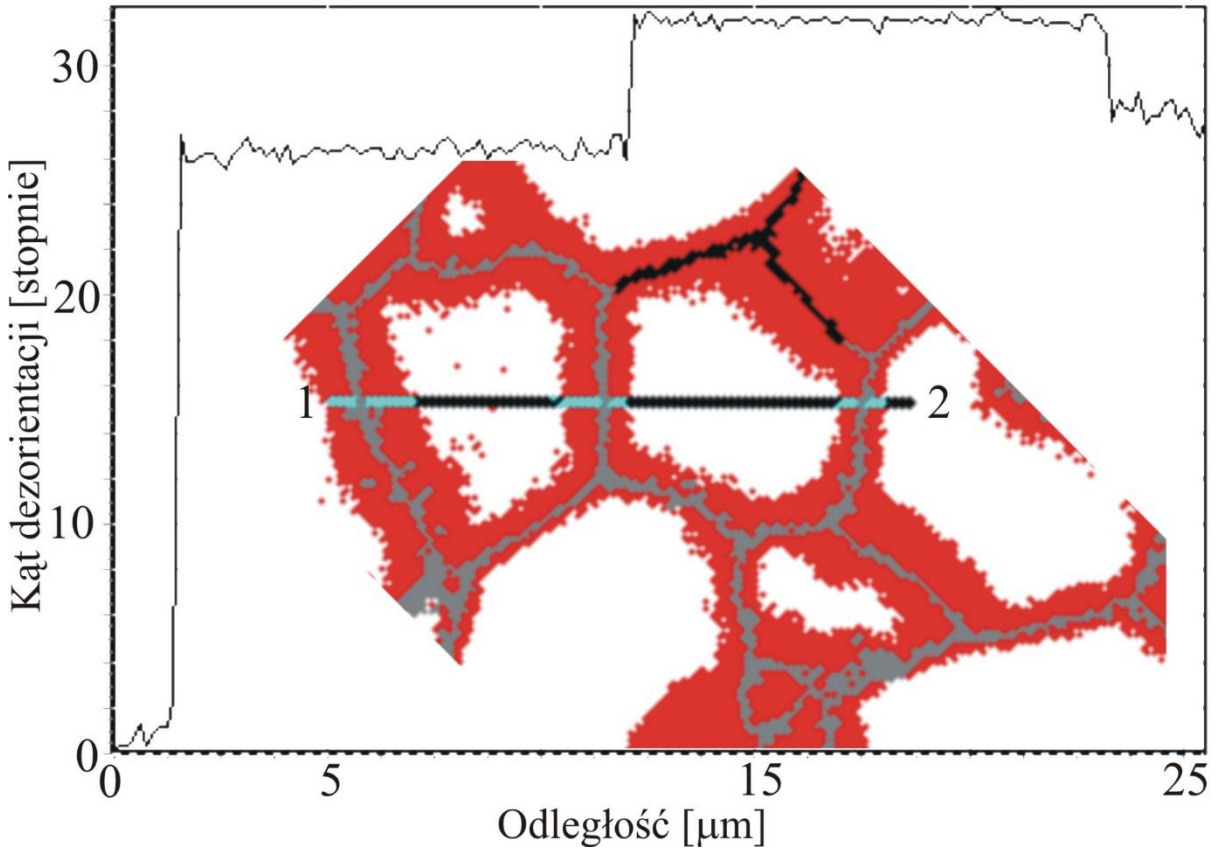

Polycrystalline zinc (99,995%) has very low mechanical properties at room temperature in spite of the plastic deformation carried out until fracture. With a grain size of about 40 μm, $R_{0,2} \approx 40$ MPa, $R_m \approx 110$ MPa.

If, however, the plastic deformation of zinc will be carried out in the scheme preventing destruction (SPD methods), it can carry much higher strain than conventionally applied, reaching $R_{0,2} \approx 160$ MPa and $R_m \approx 170$ MPa. Such a strong mechanical effect is due to the fragmentation of the zinc grains to nanometer size, practically in the absence of dislocations. The importance of point defects is neglected due to the very low concentration.

The concept of combining high strength properties with grains fragmentation fails in relation to zinc extruded by KOBO method. The process carried out at room temperature, with the extrusion ratio of $\lambda = 25$ (diameter of the charge 40 mm) and a speed of 0.5 mm/s and die oscillating at an angle ± 8 ° at a frequency of 5 Hz, results in receiving a product which $R_{0,2} \approx 150$ MPa while $R_m \approx 250$ MPa, wherein the average grain size is of several dozen micrometers (~20 μm).

In addition, depending on the value of the extrusion parameters applied, zinc stretching curves re characterized by - leading to destruction - immediate mechanical instability, reveal Lüders phenomenon or run smoothly, the same way as metals in recrystallized state.

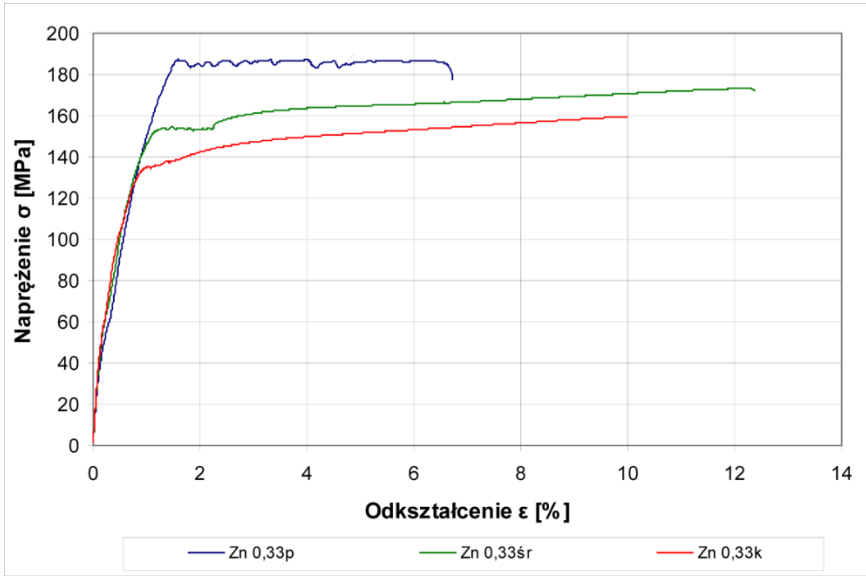

Mechanical characteristics of "cold" extruded zinc by KOBO method with the degree of processing of $\lambda = 100$, stamp speed of 0.33 mm / s, at an angle of oscillating movement of die equal to ± 8 °, depending on the magnitude of the extrusion force applied (regulated by frequency of die oscillations).

Microstructure (IPF map) of initial state of zinc, SEM/BSD.

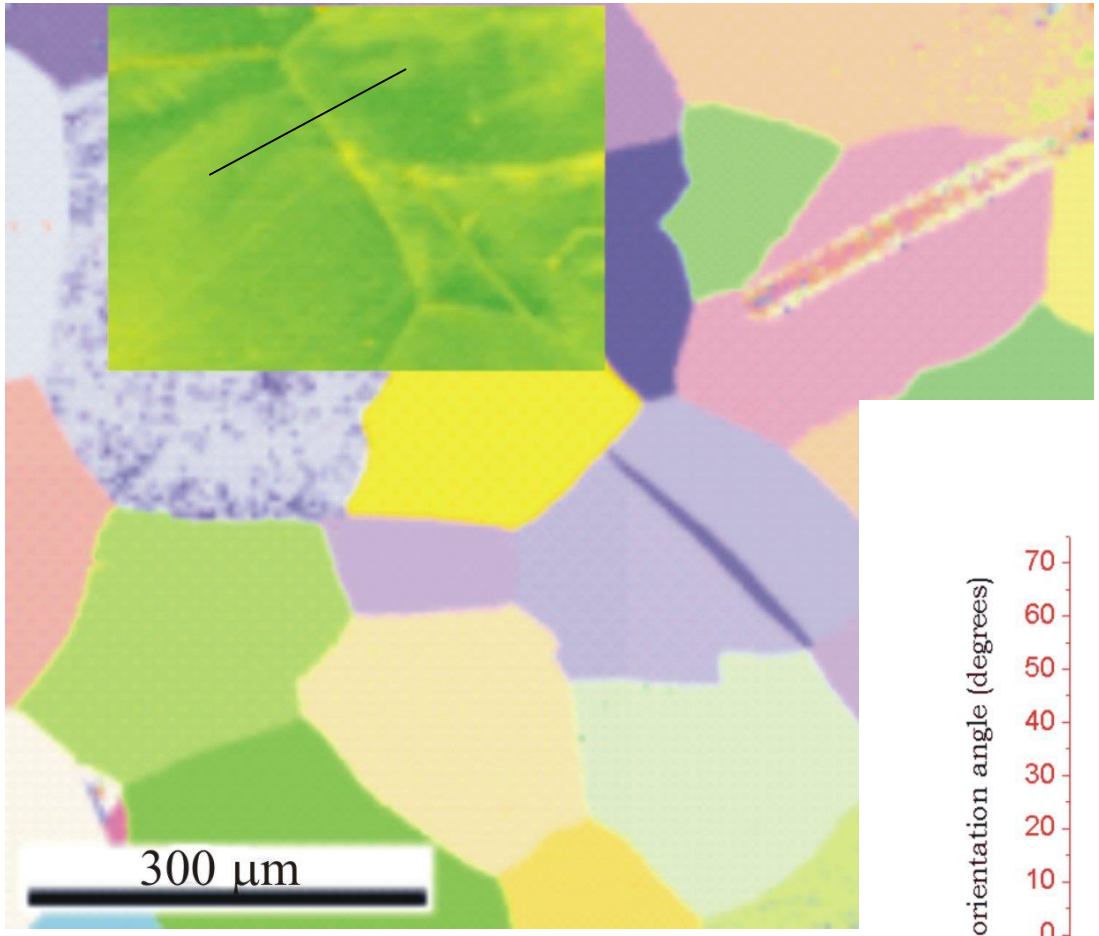

Expanded area map shows distribution of IQ factor: green – high IQ value, yellow – low IQ value

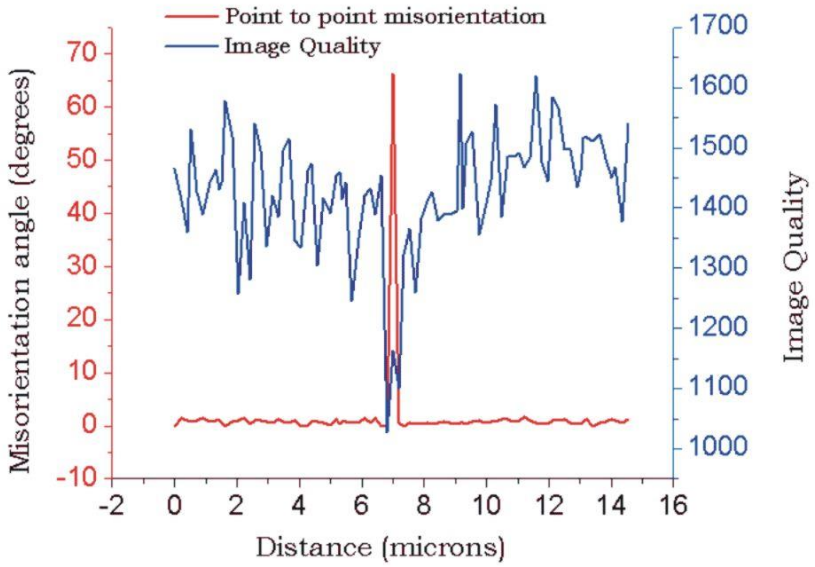

Cross section through HAGB showing variation of IQ factor (blue line) and point to point misorientation angle (red line) in initial sample.

Transverse section of KoBo extruded zinc wire, scan taken along radius of the wire.

a) IQ factor map from values color coded:

green – high IQ,

yellow – medium,

red – low IQ,

HAGBs indicated with black line.

b) IPF map, intergranular bands indicated with arrows.

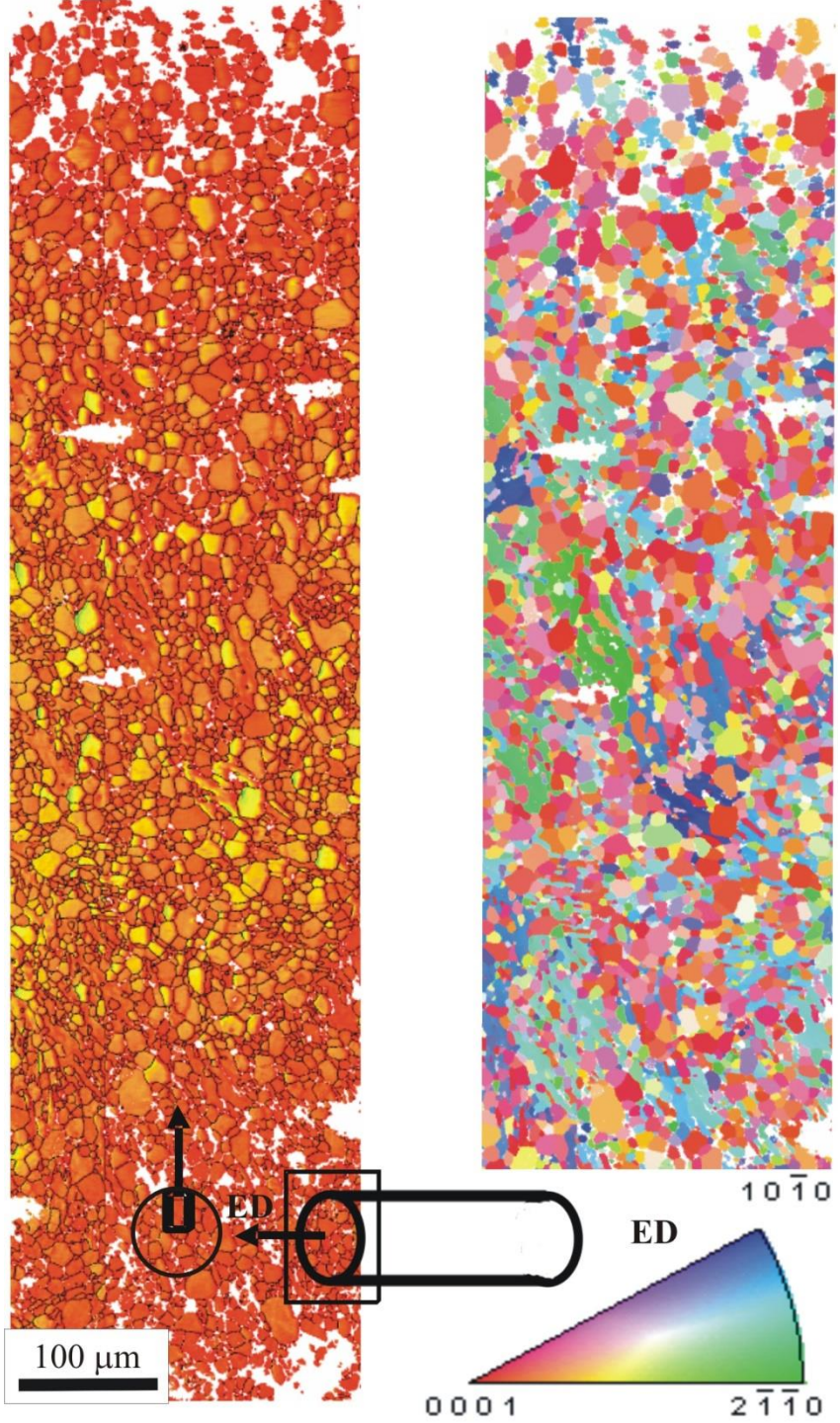

Longitudinal section of KoBo extruded zinc wire, scan taken along radius of the wire.

a) IQ factor map from values color coded:

green – high IQ,

yellow – medium,

red – low IQ,

HAGBs indicated with black line.

b) IPF map, intergranular bands indicated with arrows.

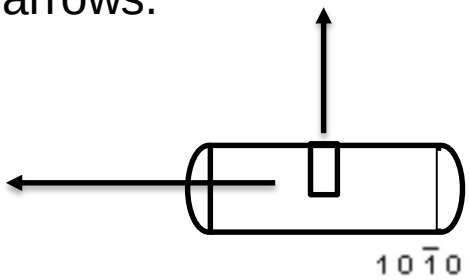

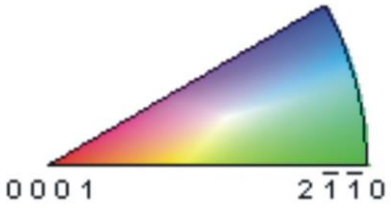

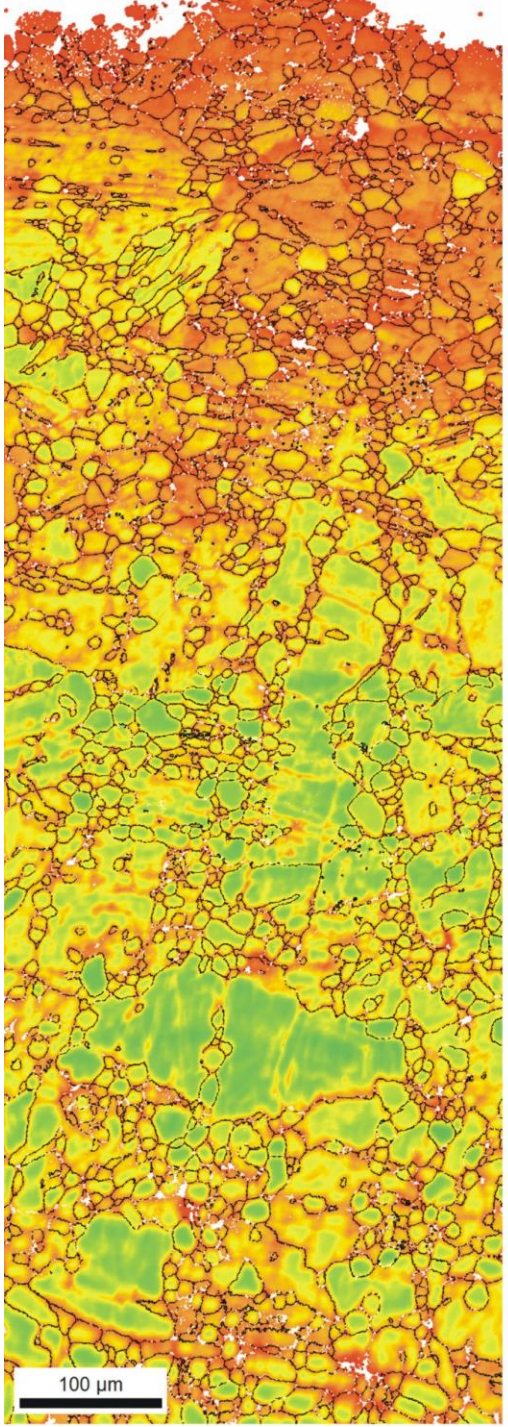

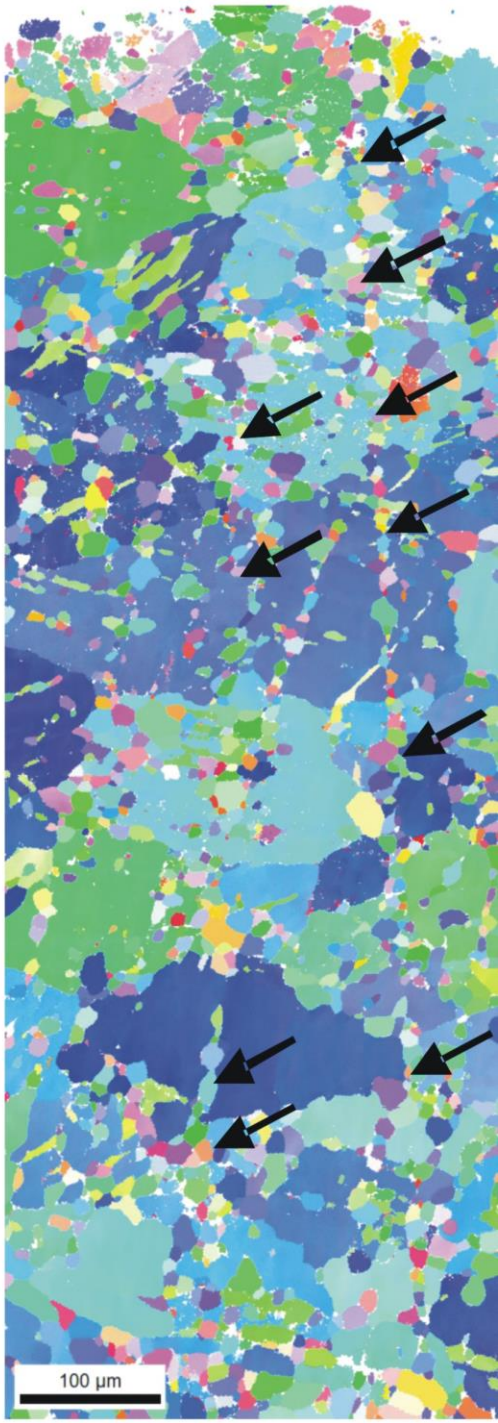

Texture of zinc after KoBo extrusion

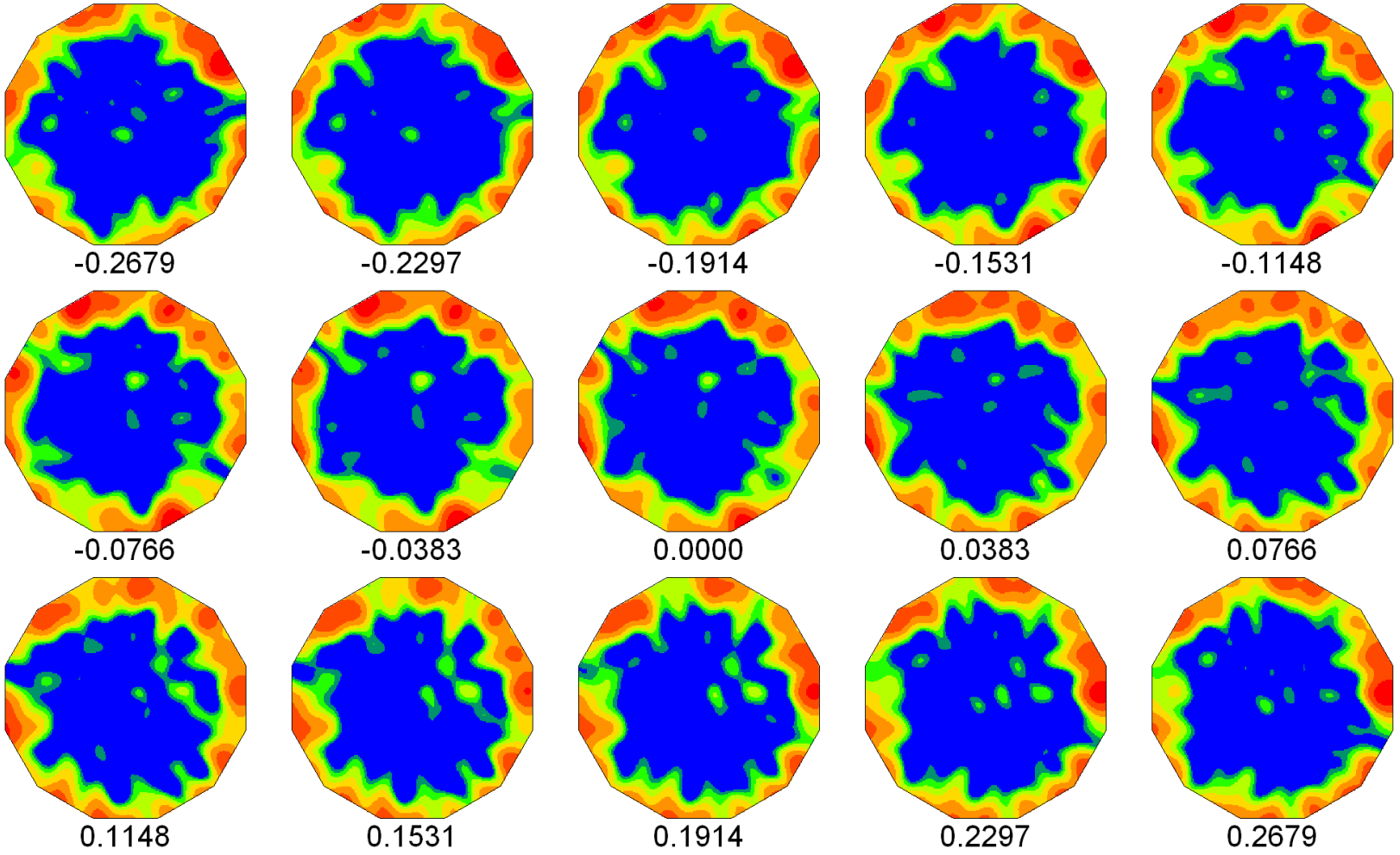

An example of Orientation Distribution Function, Rodrigues' representation r_1, r_2, r_3, cross-section r_3=const., asymmetric domain (D_6).

Cross section through HAGB showing variation of IQ factor

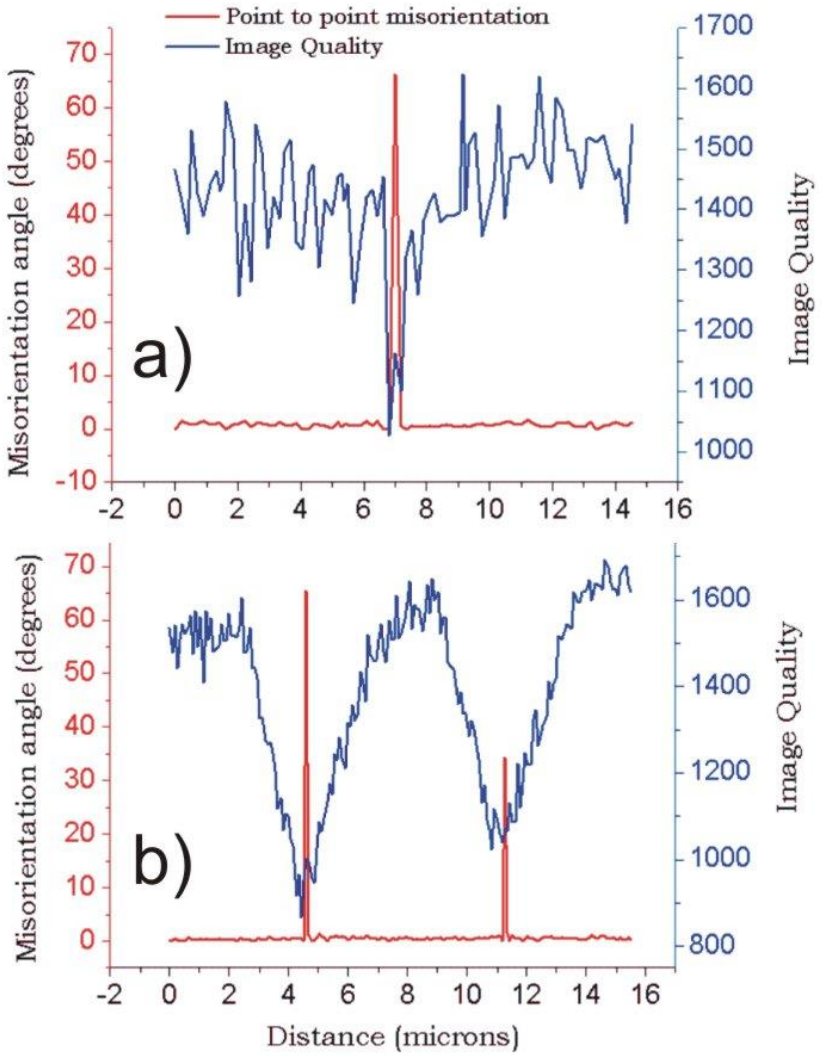

- IQ - blue line
- point to point misorientation angle - red line.

a) initial sample;

b) KoBo extruded sample.

Microstructure of zinc after KoBo extrusion

Regions with highly deformed crystal lattice (low values of IQ factor) are indicated with red colour. Insides of grains with low density of defects are presented by white areas. HAGBs marked with black lines. Point to origin misorientation angles along cross section (points A to B) through two typical grains are presented.

A

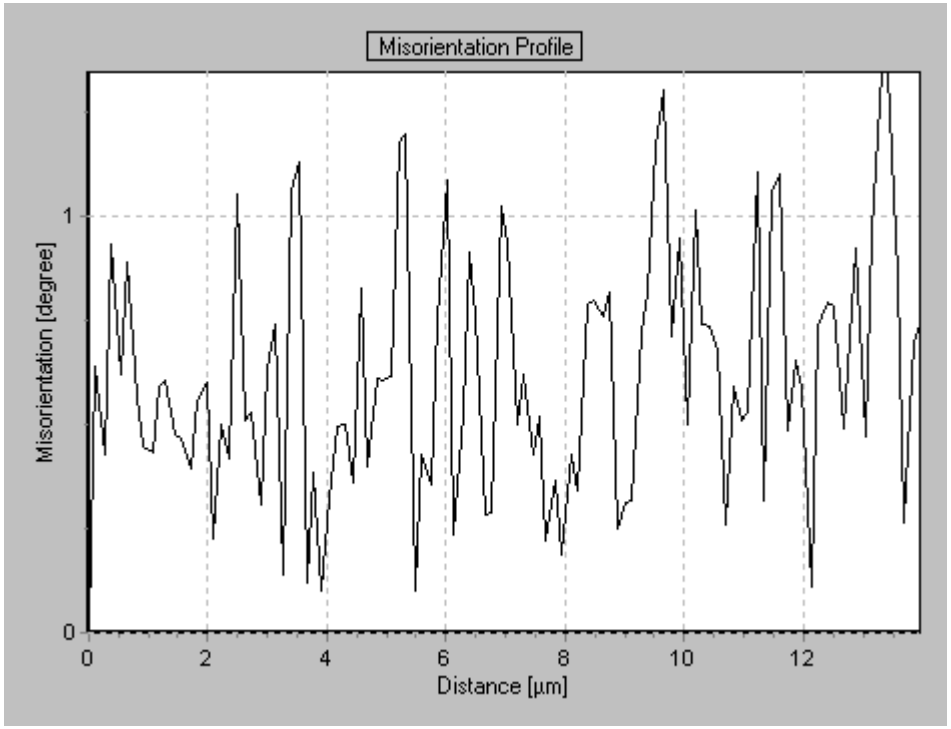

B

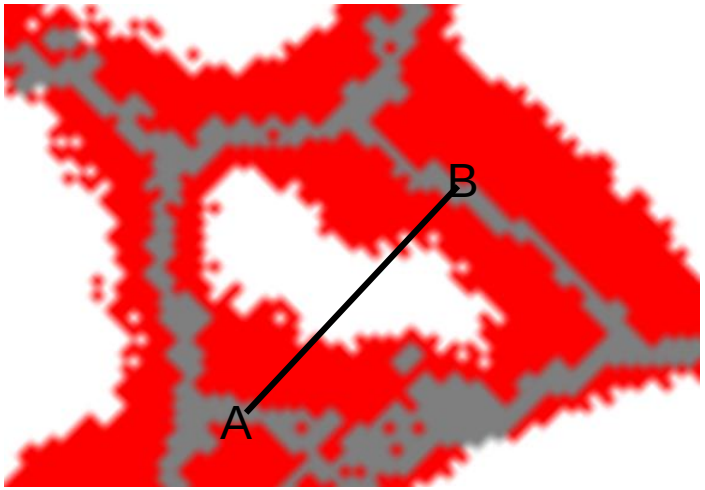

Microstructure of zinc after KoBo extrusion

Subtle misorientation changes in the bent crystal/grain.

b) Point to origin misorientation variation profile (points 3-4) indicates curvature of lattice realized by geometrically necessary dislocations (GNDs)

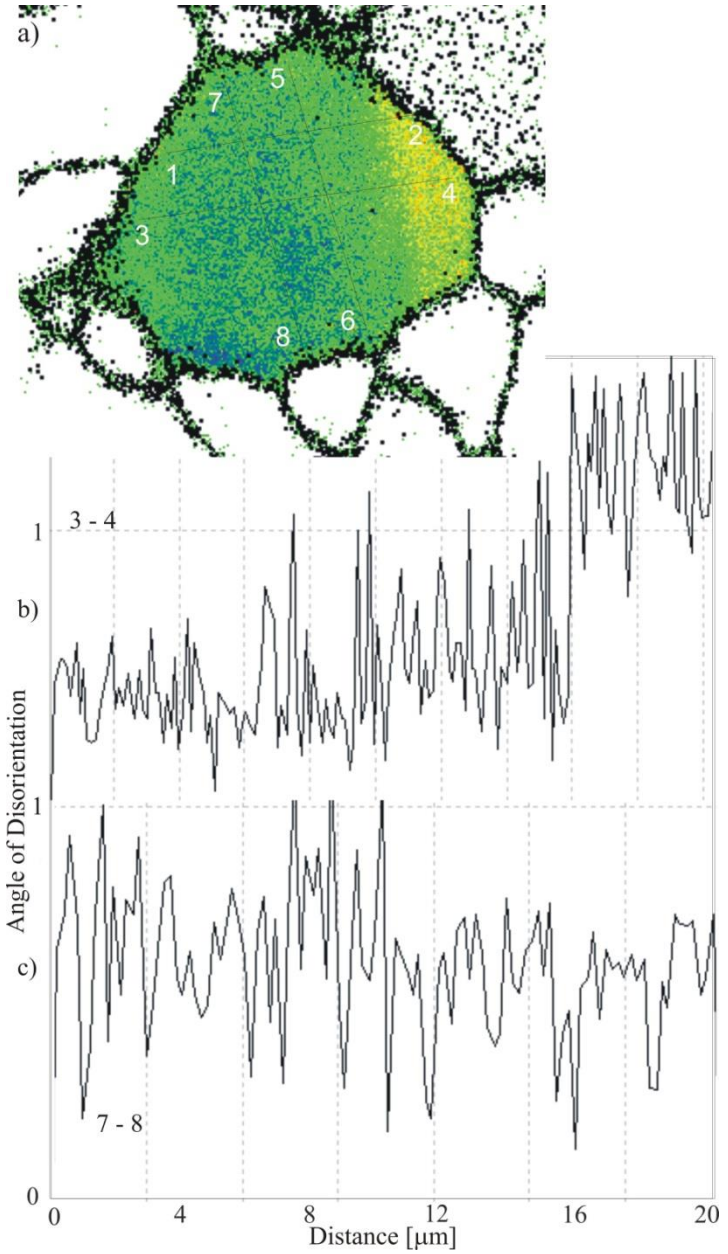

Microstructure of zinc after KoBo extrusion

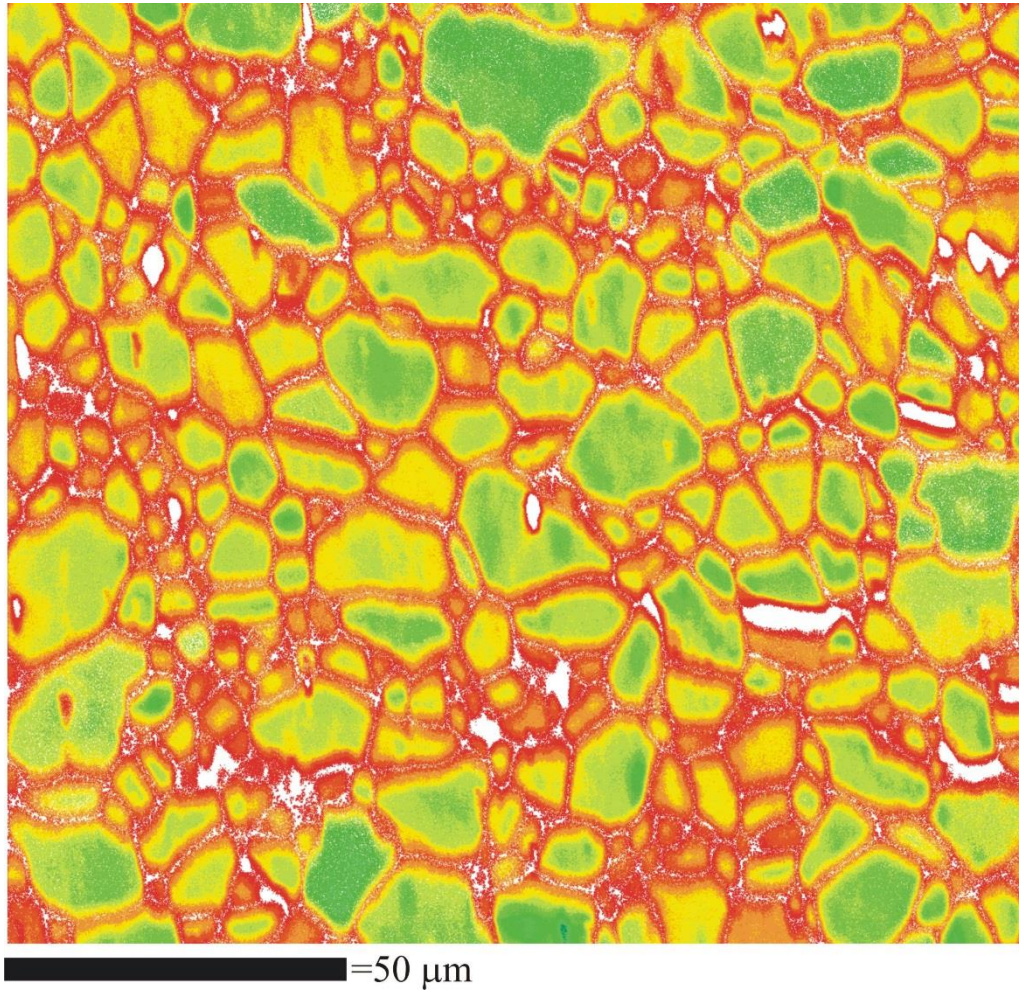

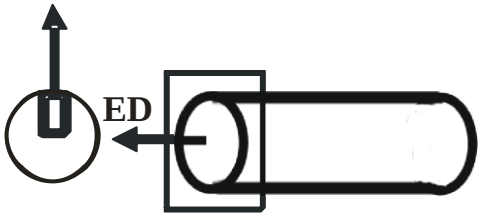

IQF topography

The deformed areas of the crystal lattice extending along the HAGBs occupy of ~30% of the volume of material within the sample and ~60% in the surface layer.

Microstructure of zinc after KoBo extrusion

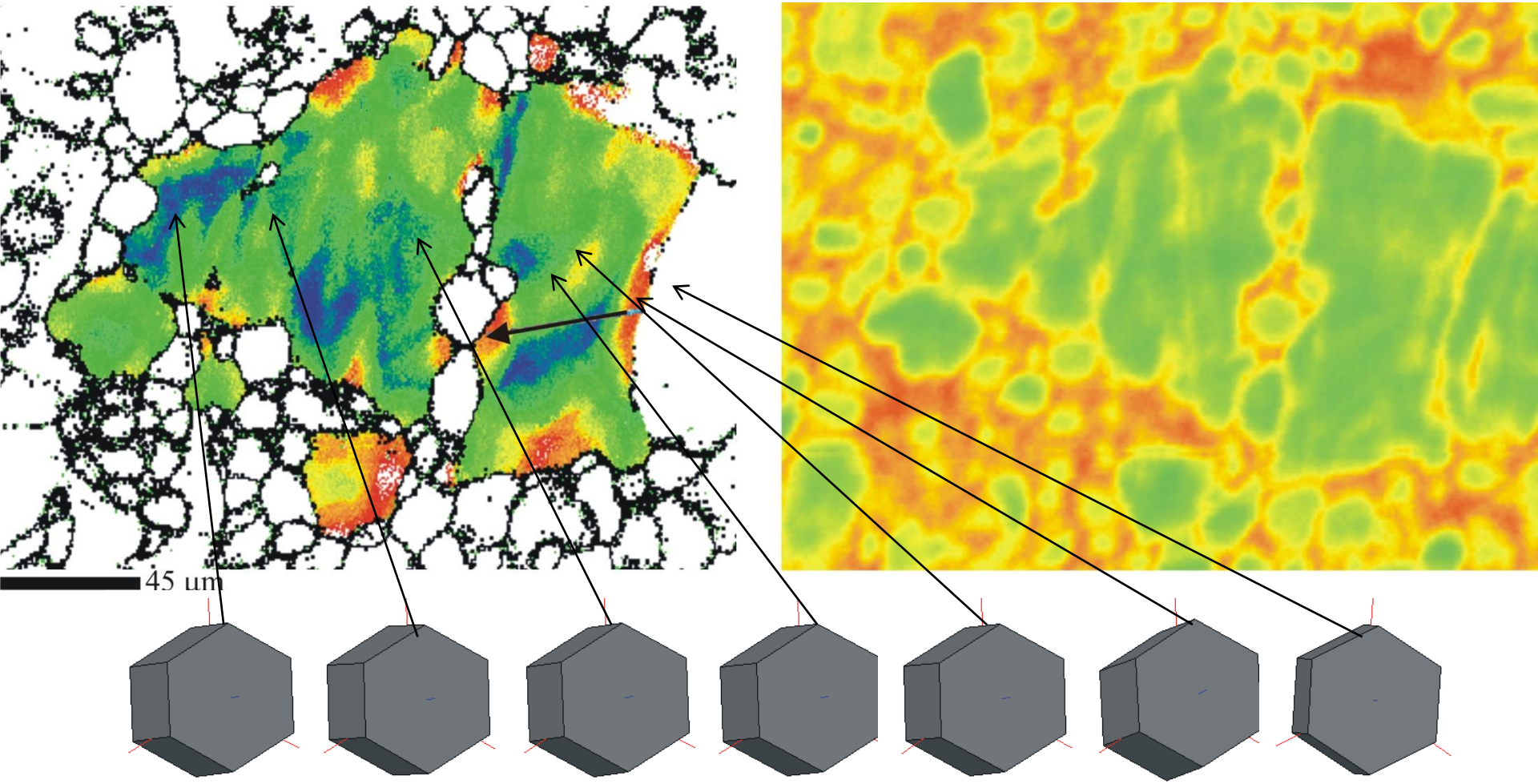

Large, partialy fragmented primary grain. Left: Orientation fluctuations inside grain; misorientation angle in respect to selected basal orientation is colour coded: blue 0, green 2, red 4. Right: Topography of crystal lattice defect concentration

Microstructure of zinc after KoBo extrusion

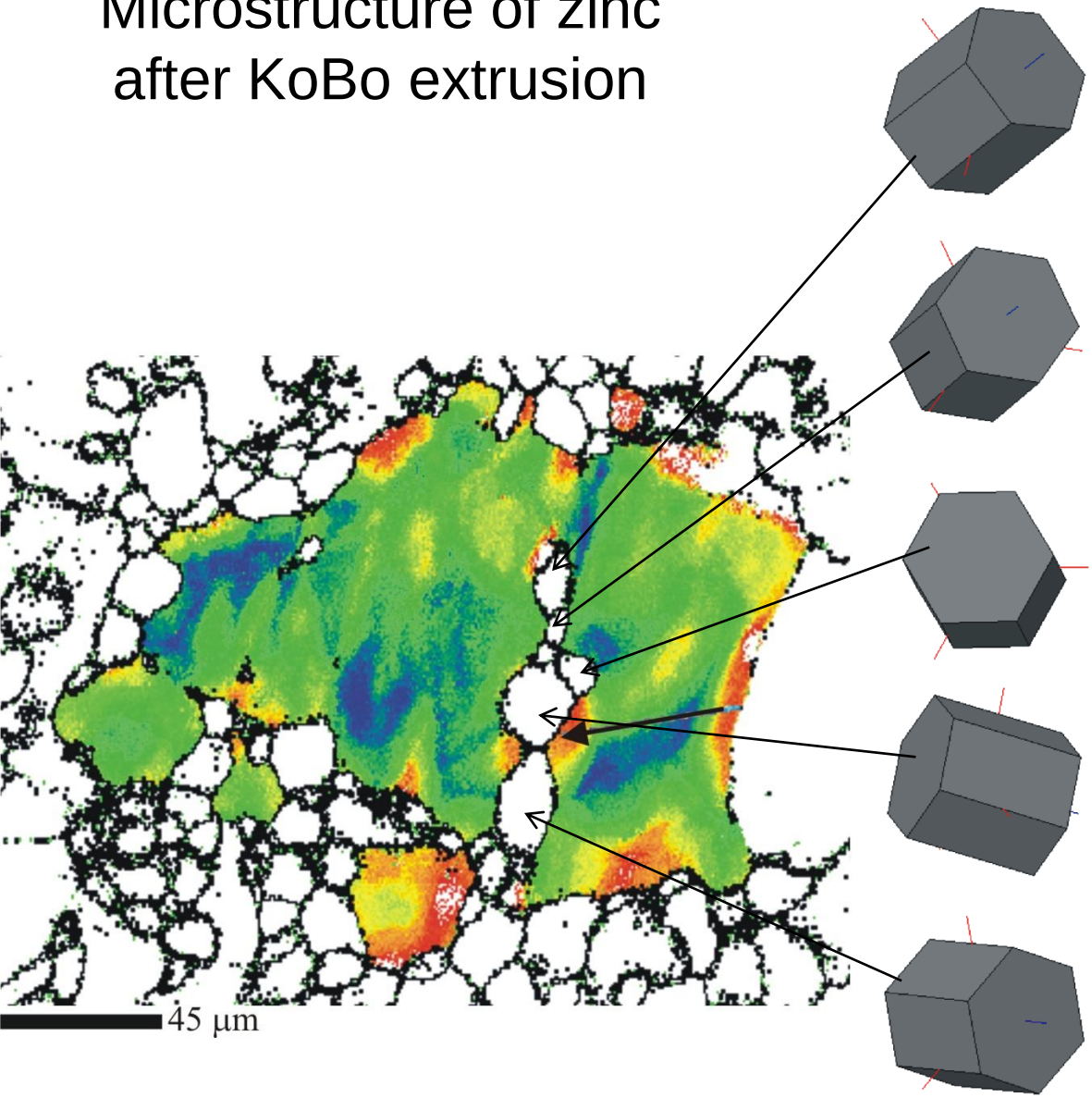

Large, partialy fragmented primary grain. Left: Orientation fluctuations inside grain, Misorientation angle in respect to selected basal orientation is colour coded: blue 0, green 2, red 4. Arrows indicates fine recrystallized grains forming a band. Right: Topography of crystal lattice

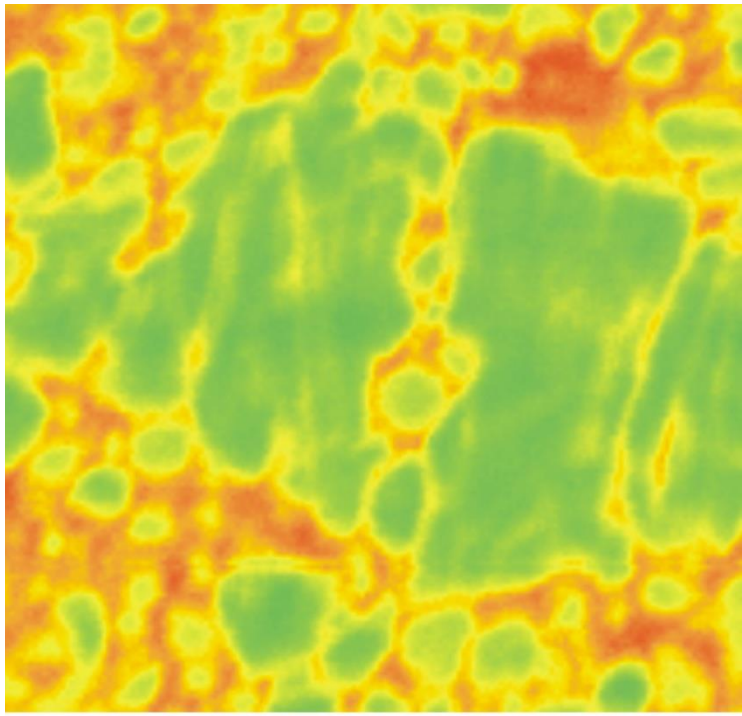

Thank you